NOAA Technical Memorandum ERL WPL-10

U.S. DEPARTMENT OF COMMERCE
NATIONAL OCEANIC AND ATMOSPHERIC ADMINISTRATION
Environmental Research Laboratories

A Feasibility Study of an Optical Crosswind Monitor

G.R. OCHS
S.F. CLIFFORD
TING-I WANG

Wave
Propagation
Laboratory
BOULDER,
COLORADO
September 1973

ENVIRONMENTAL RESEARCH LABORATORIES

WAVE PROPAGATION LABORATORY

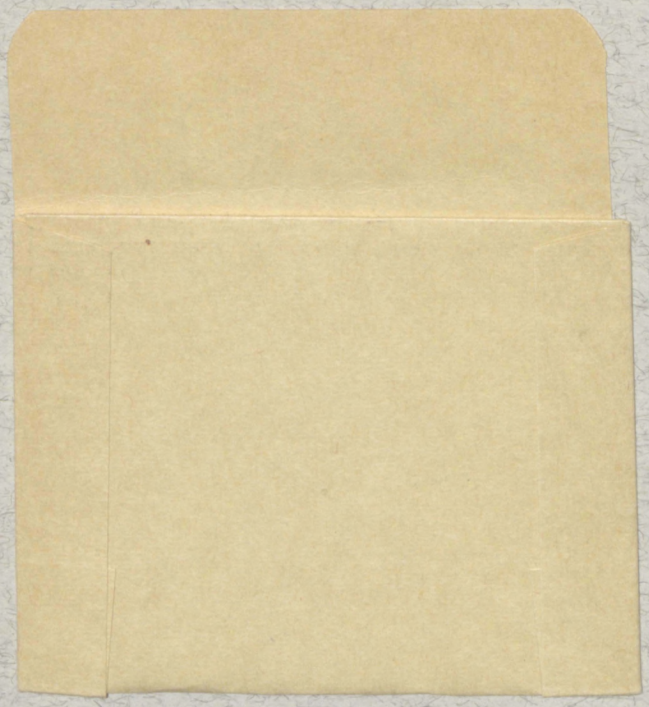

IMPORTANT NOTICE

Technical Memoranda are used to insure prompt dissemination of special studies which, though of interest to the scientific community, may not be ready for formal publication. Since these papers may later be published in a modified form to include more recent information or research results, abstracting, citing, or reproducing this paper in the open literature is not encouraged. Contact the author for additional information on the subject matter discussed in this Memorandum.

NATIONAL OCEANIC AND ATMOSPHERIC ADMINISTRATION

BOULDER, COLORADO

U.S. DEPARTMENT OF COMMERCE
National Oceanic and Atmospheric Administration
Environmental Research Laboratories

NOAA Technical Memorandum ERL WPL-10

A FEASIBILITY STUDY OF AN OPTICAL CROSSWIND MONITOR

G. R. Ochs and S. F. Clifford
National Oceanic and Atmospheric Administration
Environmental Research Laboratories
Boulder, Colorado 80302

and

Ting-i Wang
Cooperative Institute for Research in the Environmental Sciences
Boulder, Colorado 80302

This research was supported in part by the
Army Electronics Command, Atmospheric Sciences
Laboratory, White Sands, N. M. 88002,
under MIPR A43bxl 73 80 16. Mr. T. H. Pries
was the ASL Scientific Monitor

Wave Propagation Laboratory
Boulder, Colorado
September 1973

TABLE OF CONTENTS

A FEASIBILITY STUDY OF AN OPTICAL CROSSWIND MONITOR

G. R. Ochs, S. F. Clifford, and Ting-i Wang*

This report summarizes progress to date on our feasibility study of a laser-beam crosswind-measuring system. In the first section, we consider the laser system concept and discuss its limitations, namely the uncontrollable variability of the path-weighting function and its tendency to peak at less than 10 percent of the path from the transmitter in high refractive turbulence. In the second section, we consider an alternative approach called the "passive" system that uses the naturally occurring, ambient illumination of the target to extract wind information. This technique has the advantage that, unlike the laser system, at least from the point of view of the first-order theory, the path-weighting functions are independent of the level of refractive turbulence and exhibit a reasonable degree of variability with changes in detector spacing. Also included in appendix A are some recent results on the saturation problem. It is quite likely that the effects of saturation will have some influence on both the laser and passive techniques. The size of these effects on the wind-weighting functions has yet to be evaluated.

1. INTRODUCTION

During the period from November 1, 1972, to September 30, 1973, we conducted a theoretical and experimental study of the feasibility of a laser-beam crosswind monitor. The system as initially posed consisted of a laser transmitter and a collocated set of receiving optics. The principle of operation of this single-ended system was that a receiver telescope would observe a laser-illuminated target; from an analysis of the atmospherically induced fluctuations in the pattern of illumination (scintillation pattern), information about the crosswind along the path could be derived. The first part of this report is a detailed analysis of the system and a conclusion as to its feasibility. In the second part, we consider an alternative approach and its relative merits.

*Ting-i Wang is with the Cooperative Institute for Research in the Environmental Sciences, an institute sponsored jointly by the University of Colorado and the National Oceanic and Atmospheric Administration.

2. ANALYSIS OF THE LASER-BEAM SYSTEM

To understand the single-ended system, it is convenient to consider scintillation effects on the two legs of the folded path separately. These will be called the target-illuminating and target-return links, respectively. In figure 1, the former is from A to B and the latter from B to A, with both paths nearly coincident and immersed in turbulent temperature fluctuations. For the purposes of analysis, we consider the laser as a point source of monochromatic light. The analysis of any other model, for example, a distributed source, is found by a weighted linear combination of the point source results.

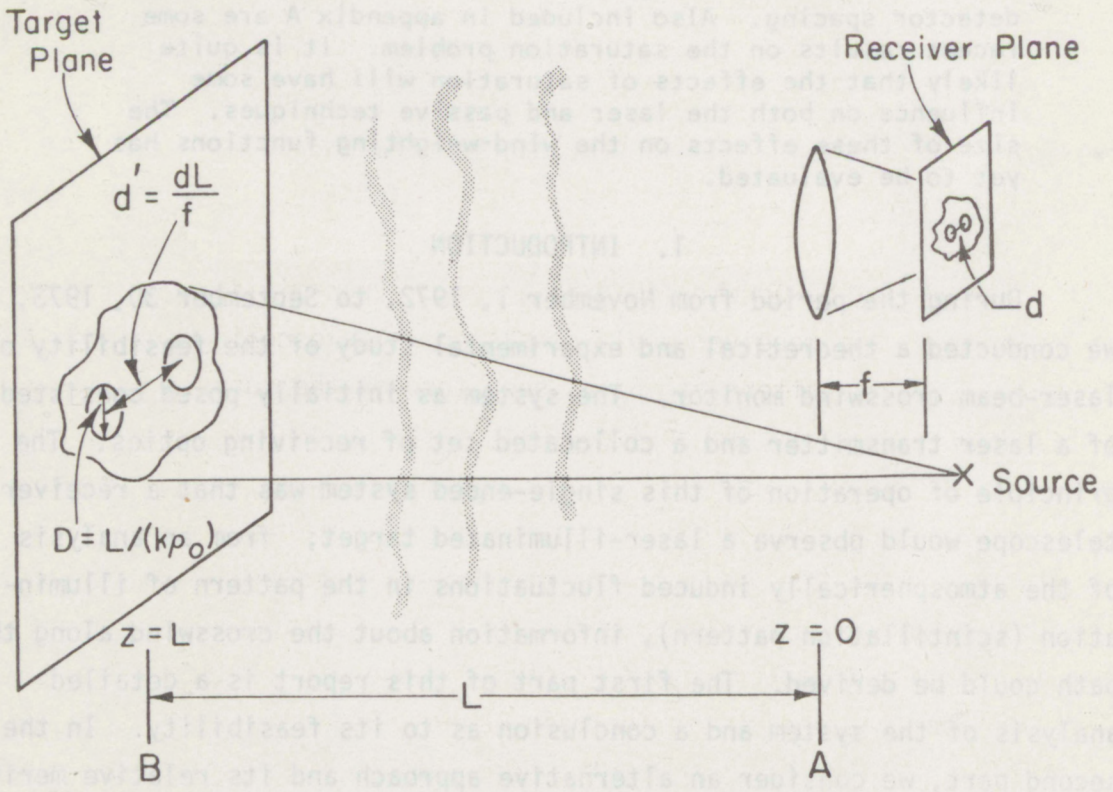

Figure 1. The propagation geometry for the laser-beam crosswind-measuring system.

The point source at A emits a spherical wave that endures phase perturbations produced by wind-driven temperature irregularities advected through the beam. These phase fluctuations eventually cause adjacent rays to interfere, producing an irregular distribution of irradiance at the target. This so-called scintillation pattern evolves in time as the result of changes in the wind velocity, allowing us to extract wind information by applying statistical analysis to the signal in the target plane at B. This particular propagation problem, that is, the target-illuminating link, has been extensively treated by Clifford (1971), Lawrence, Ochs, and Clifford (1972), and by Ochs and Miller (1972).

As described by Lawrence, Ochs, and Clifford (1972), we have already developed a double-ended wind-sensor system involving a two-point correlation technique (see also Ochs and Miller, 1972) that can analyze the signal at B and extract a path-weighted average wind. This weighting function can be varied from nearly flat to one that emphasizes the wind near either the transmitter or the receiving plane. As first envisaged, the single-ended wind sensor would extract the wind information that exists on the signal at B and would try to ignore the noise produced by the same wind-driven turbulence on the target-return link. This might be accomplished by a set of transmitting and receiving optics at A; the receiver would consist of a telescopic lens to view the scintillation pattern at B, as seen through the turbulent atmosphere on the return link, and to analyze that pattern with a two-point wind sensor at the focal plane. If the distortion of the scintillation pattern on the return link does not degrade the wind information imposed on the illuminating link, the average wind could be extracted as easily as is done with a double-ended system. The telescope would merely reduce the size of the target pattern by the ratio f/L, where f is the focal length of the lens and L is the path length BA.

Unfortunately, the intervening turbulent medium distorts the target scintillation pattern on the return link and degrades the wind information that the pattern contains. Figure 1 illustrates this problem. The minimum resolvable length in the target plane at B, viewed from A, is

$\sim L/k\rho_0$ (Fried, 1966; and Lutomirski and Yura, 1971), where L is the length of the intervening turbulent medium, k is the wavenumber of the visible radiation, and ρ_0 is the transverse distance over which the mutual coherence function (Lutomirski and Yura) falls to e^{-1} times its maximum value. For our propagation problem, ρ_0 is equivalent to the phase coherence length that is defined as the transverse distance over which the rms phase-deviation of a spherical wave, emitted at B and arriving at A, is less than 1 rad. This resolution limit implies that the smallest detail in the pattern at B, observable from A, is of size $L/k\rho_0$. Therefore, measuring the crosswind with two point detectors separated by a distance d in the focal plane of a lens at A is equivalent to using two detectors of diameter $D = L/k\rho_0$ separated by a distance $d' = dL/f$ in the target plane at B. The theoretical analysis is then simplified to the line-of-sight problem considered in an earlier work (Lawrence, Ochs, and Clifford, 1972), with the added complication of aperture-averaging effects.

3. THEORY

To compute the effects of using finite apertures rather than point detectors, we follow the earlier analysis of Fried (1967). Physically, it is immediately apparent that larger apertures will progressively average out more of the small-scale structure in the scintillation pattern and will bias the wind-weighting function more toward the transmitter end of the path where the larger scale effects originate.

Mathematically, we describe the signal s, observed by an aperture of diameter D at the position $\underset{\sim}{r}_1$ and time t, in the form

$$s(\underset{\sim}{r}_1,t) = \int d^2\underset{\sim}{\rho}'\ W(\underset{\sim}{\rho}',D)\ I(\underset{\sim}{r}_1+\underset{\sim}{\rho}',t), \tag{1}$$

where I is the irradiance that varies as a function $\underset{\sim}{\rho}'$ in the xy-plane (see fig. 2). Using equation (1), we construct the space-time covariance function in the form

$$W(\underset{\sim}{\rho}', D) = \begin{cases} 1 & \rho' \leq D/2 \\ 0 & \rho' > D/2 \end{cases}, \tag{2}$$

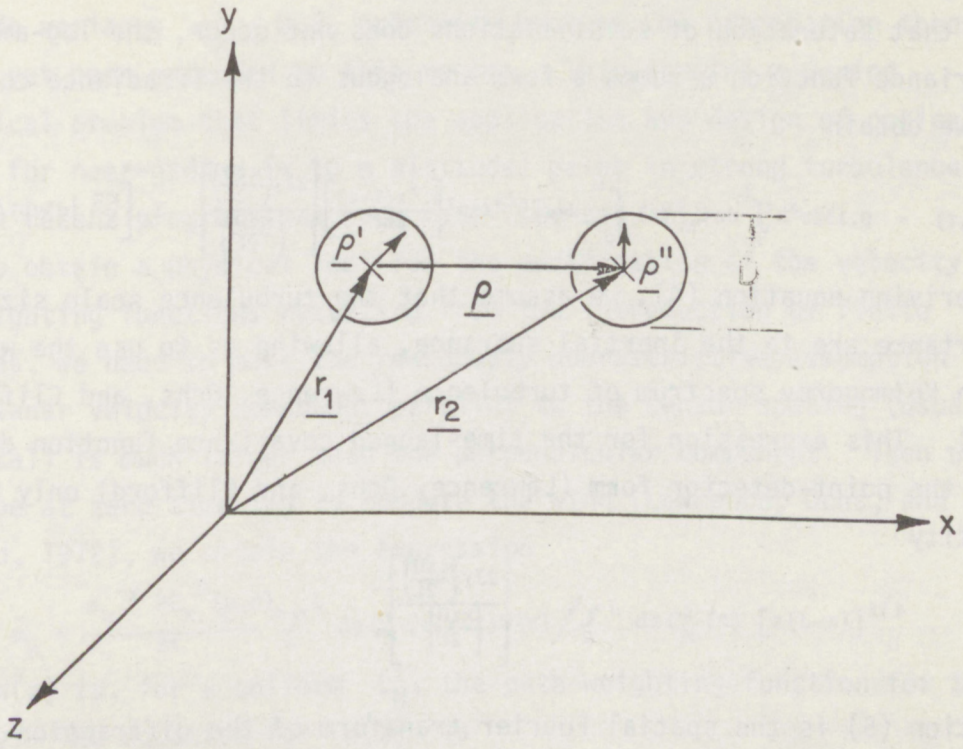

Figure 2. Coordinate system and a definition of the geometric quantities found in equation (17).

where D is the aperture diameter. The incident laser signal is represented as a spherical wave propagating along the z-axis. As it travels, the wave encounters a nonuniform distribution of refractive turbulence $C_N^2(z)$ that is moving through the beam with a transverse velocity $v(z)$. Using equation (1), we construct the space-time covariance function in the form

$$C_s(\underset{\sim}{\rho}, \tau) = \langle s(\underset{\sim}{r}_1, t)\, s(\underset{\sim}{r}_1 + \underset{\sim}{\rho}, t+\tau) \rangle , \qquad (3)$$

where the angle brackets indicate an ensemble average. After following the analogous steps to those in Fried's work (1967), with minor complications resulting from the additional time variation and the assumption of a spherical rather than a plane incident wave (these effects are described in detail by Clifford (1971)), we eventually arrive at the aperture-averaged covariance of the irradiance fluctuations. For the case when

the Rytov assumption applies, that is, when the turbulence is sufficiently weak that saturation of scintillations does not occur, the log-amplitude covariance function assumes a form analogous to the irradiance covariance, and we obtain

$$C_\chi^D(\underset{\sim}{\rho},\tau) = 0.132\pi^2k^2\int_0^L dz\, C_N^2(z)\int_0^\infty d\kappa\kappa^{-8/3}\sin^2\left[\frac{\kappa^2 z(L-z)}{2kL}\right]\left[\frac{2J_1\left(\frac{\kappa zD}{2L}\right)}{\left(\frac{\kappa zD}{2L}\right)}\right]^2 J_o\left[\frac{\kappa z}{L}\,|\underset{\sim}{d}-\underset{\sim}{v}L\tau/z|\right]. \quad (4)$$

In deriving equation (4), we assume that the turbulence scale sizes of importance are in the inertial subrange, allowing us to use the well-known Kolmogorov spectrum of turbulence (Lawrence, Ochs, and Clifford, 1972). This expression for the time-lagged covariance function differs from the point-detector form (Lawrence, Ochs, and Clifford) only by the quantity

$$\left[\frac{2J_1\left(\frac{\kappa zD}{2L}\right)}{\left(\frac{\kappa zD}{2L}\right)}\right]^2. \quad (5)$$

Equation (5) is the spatial Fourier transform of the diffraction-limited modulation transfer function (mutual coherence function) of an imaging system with a circular aperture.

The argument of the first-order Bessel function J_1 is a function of $\kappa z/L$ and is not merely the turbulence wavenumber κ because we assumed an incident spherical wave. The received image of a turbulent eddy at path position z is scaled in size by the factor L/z resulting from the divergence of the ray bundle leaving the source. Hence $\kappa z/L$ represents, in effect, the spatial wavenumber of the Fourier components of the received pattern itself. Note in the limit $D \to 0$, equation (4) returns to the form found earlier (Lawrence, Ochs, and Clifford, 1972).

Equation (4) is a rather complicated expression that describes the log-amplitude covariance function of a spherical wave propagating through a medium with a nonuniform C_N^2 and velocity profile. The velocity vector may assume any angle with respect to the plane that contains A and B and the line adjoining the centers of the two apertures of arbitrary diameter D. The only significant limitation of equation (4) is that it is not valid for strong scintillations, that is, a log-

amplitude variance $\sigma_\chi^2 \geq 0.3$, primarily because the propagation theory has not yet been extended to this regime. This remains a vexing theoretical problem that limits the application and design of optical systems for near-ground (< 10 m altitude) paths in strong turbulence, although recent progress has been made (see app. A).

To obtain a physical feel for the modification of the velocity path-weighting functions resulting from the introduction of finite apertures, we need to make the reasonably nonrestrictive assumption that the coplanar velocity component parallel to the sensor spacing (usually horizontal) is much larger than the perpendicular component. Then using the slope at zero time-lag to compute the wind (Lawrence, Ochs, and Clifford, 1972), we obtain the expression

$$m_n = \frac{\sigma_x^{-2}\,\partial C_x^D(\underset{\sim}{\rho},o)}{\partial\tau} = \int_o^L dz\, C_N^2(z)v(z)W(z) \Big/ \int_o^L dz\, C_N^2(z)\,[z(L-z)]^{5/6}\,, \qquad (6)$$

where $W(z)$ is, for a uniform C_N^2, the path-weighting function for the velocity. The equation for $W(z)$ is

$$W(z) = 2.33(kL)^{5/6}\int_o^\infty d\kappa\kappa^{-5/3}\sin^2\left[\frac{\kappa^2 z(L-z)}{2kL}\right] J_1\left(\frac{\kappa d' z}{L}\right)\left[\frac{2J_1\left(\frac{\kappa zD}{2L}\right)}{\left(\frac{\kappa zD}{2L}\right)}\right]^2 . \qquad (7)$$

The change of variables to $y = \kappa z\sqrt{\frac{\lambda}{L}}$ and $u = z/L$ will greatly facilitate the physical interpretation of equation (7). This results in the expression

$$W(u) = 4.30k^{3/6}L^{7/6}u^{2/3}\int_o^\infty dy\, y^{-5/3}\sin^2\left[\frac{y^2\left(\frac{1}{u}-1\right)}{4\pi}\right] J_1(d_n' y)\left[\frac{2J_1\left(\frac{yD_n}{2}\right)}{\left(\frac{yD_n}{2}\right)}\right]^2, \qquad (8)$$

where $d_n' = d/\sqrt{\lambda L}$ and $D_n = D/\sqrt{\lambda L}$.

We must now relate the parameters in our model, equation (8), to those relevant to our path geometry (fig. 1). From the above discussion, d' for the single-ended measurement scheme is given by $d' = dL/f$, and consequently $d_n' = (d/f)\sqrt{L/\lambda}$. The quantity $D_n = (L/k\rho_o)(\sqrt{\lambda L})^{-1}$ when simplified becomes

$$D_n = \frac{\sqrt{L/k}}{\sqrt{2\pi}\rho_o} \quad . \tag{9}$$

A reasonable estimate for the coherence length ρ_o, valid for paths of 1 to 3 km in moderate turbulence, may be obtained from the expression found by Yura (1971),

$$\rho_o \approx \left[0.54k^2 \overline{C_n^2} L\right]^{-3/5} \quad , \tag{10}$$

where $\overline{C_n^2}$ should be interpreted as a path average of $C_n^2(z)$ in the form

$$\overline{C_n^2} = 2.67 \int_0^1 dt\, C_n^2(t)\, t^{5/3} \quad , \tag{11}$$

where $t = 1 - z/L$, and $t = 1$ describes the transmitter-receiver end of the path. Equation (11) implies that the most effective position along the path where turbulence will most inhibit ability to resolve structure in the target plane is near the transmitter receiver. After substituting equation (10) into equation (9), we may write D_n in the form

$$D_n = 0.96\, (\overline{\sigma_x^2})^{3/5} \quad . \tag{12}$$

Figures 3 and 4 illustrate the behavior of the wind-weighting function as $\overline{\sigma_\chi^2}$ varies with a fixed sensor spacing. These curves must be questioned for the strong turbulence ($\overline{\sigma_\chi^2} \geq 0.3$) cases, both because of the uncertainties introduced by the "saturation" phenomenon and because the linear relation between irradiance and log-amplitude fluctuations is no longer true. But note that $\overline{\sigma_\chi^2}$ is the predicted variance; it will not be realized because of saturation, but nevertheless the predicted variance is the important parameter that determines the size of the effective aperture D_n. This is expected to be true even when the effects of saturation are included in the theory. The wind at the transmitter end of the path progressively becomes more important as the strength of turbulence increases. (These curves can also be interpreted as the weighting function for a double-ended wind sensor with receiving apertures of size D_n Fresnel zones.)

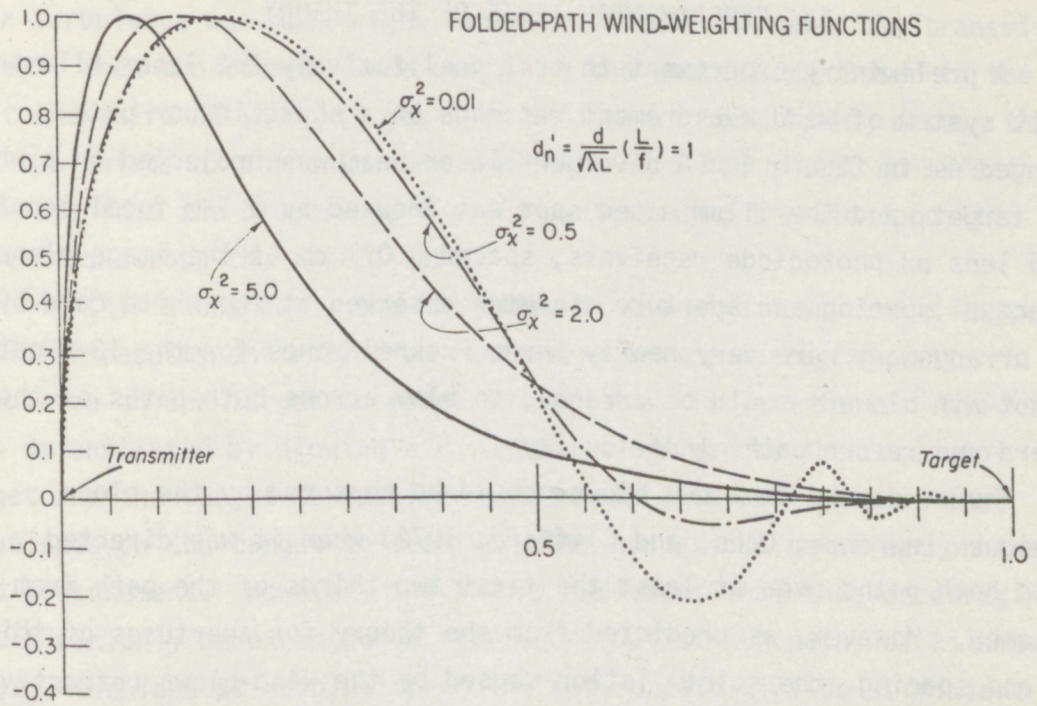

Figure 3. Wind-weighting function for a normalized spacing $d_n'=1$ Fresnel zone and strength of integrated refractive turbulence σ_χ^2.

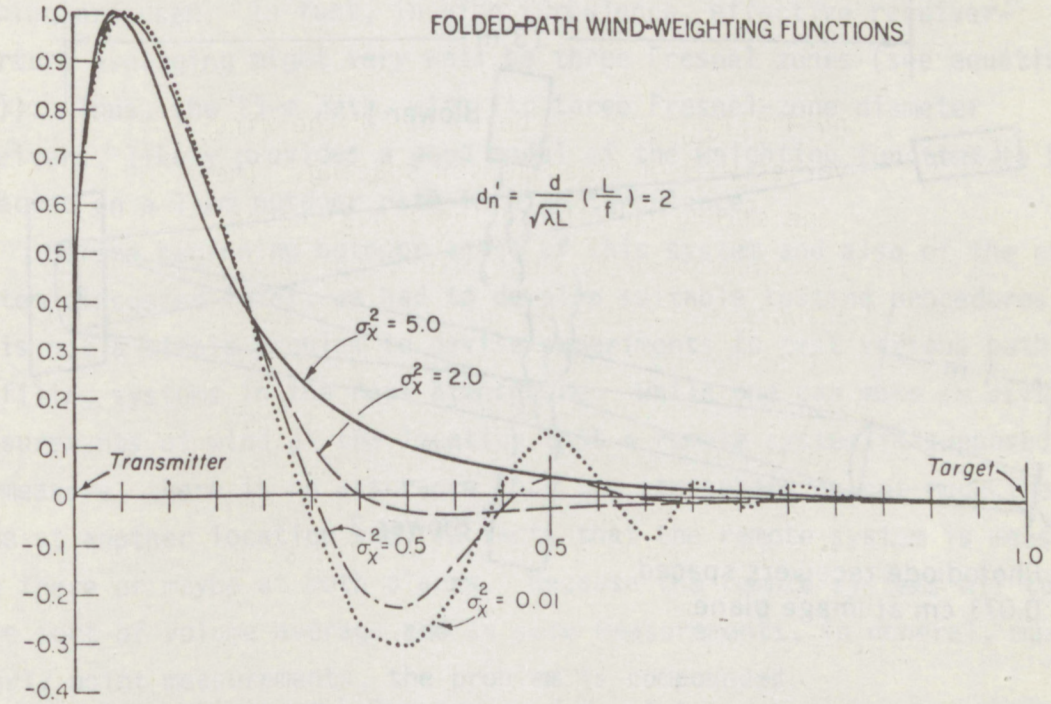

Figure 4. Wind-weighting function for a normalized spacing $d_n'=2$ Fresnel zone and strength of integrated refractive turbulence σ_χ^2.

4. EXPERIMENTAL TESTS OF THE THEORY

A preliminary experiment to test qualitatively the laser-illuminated target system of wind measurement was made on a short indoor path, arranged as in figure 5. A divergent laser beam was projected on a white card target, and the illuminated spot was focused by a 1-m focal length f.4.5 lens on photodiode receivers, spaced 0.071 cm at the image plane. The actual spacing and aperture diameter observed at the white card by this arrangement were very nearly three Fresnel zones for the 13-m path. Two hot-air blowers could be arranged to blow across both paths or the forward and return paths individually.

The windspeed from one blower could be measured by the slope technique (Lawrence, Ochs, and Clifford, 1972) when it was directed across both paths over at least the first two-thirds of the path from the laser. However, as predicted from the theory for apertures of this size and spacing, the scintillation caused by the wind-blown refractive-

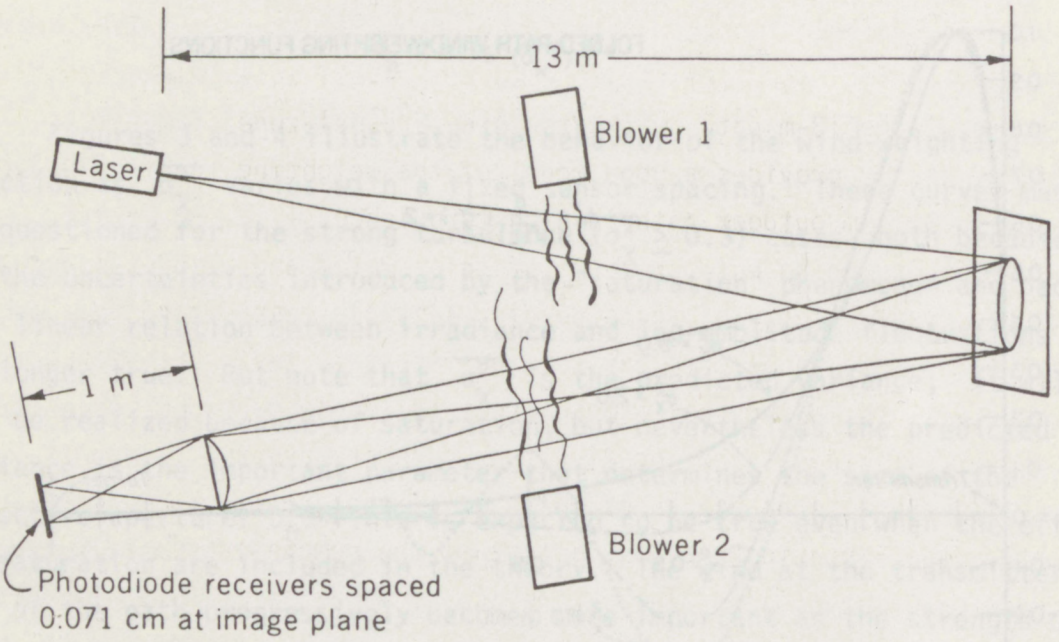

Figure 5. Experimental laser-beam crosswind-measuring system.

index turbulence was much higher when the blower was near the transmitter. In fact, when two blowers were used, the one nearest the laser in the first one-third of the path was seen while a second blowing across the last two-thirds of the path near the white card had almost no effect. The winds from the blowers were coded by directing them in opposite directions across the optical path.

On this short path, the weighting of the wind measurement toward the laser results entirely from receiver-aperture averaging, and turbulence on the target-to-receiver path has little effect. This has been demonstrated by blowing air independently across the laser-to-target and the target-to-receiver paths. In this case, we see that turbulence on the target-to-receiver path has almost no effect on the wind measurement. However, the theory indicates that this encouraging result can only be expected on very short paths. On paths of kilometer length, the loss of resolution on the return path will be sufficient in high turbulence to weight the wind measurement severely toward the transmitter-receiver end, even if very small receiver diameters and spacing are used. In fact, in high turbulence, effective receiver-aperture averaging might very well be three Fresnel zones (see equation (12)). Thus, the 13-m path, with its three Fresnel-zone diameter receivers, likely provides a good model of the weighting function to be expected on a 1-km outdoor path in high turbulence.

Before beginning outdoor tests of this system and also of the other system discussed later, we had to develop suitable testing procedures. It is not a simple problem to devise experiments to test various path-profiling systems in the real atmosphere. While one can make *in situ* measurements of wind at the location that a remote system is supposed to measure, there is no assurance that the atmosphere is not much the same at another location and, in fact, that the remote system is measuring there or maybe at both places. Because the remote systems all take some sort of volume average and *in situ* measurements, in general, must be nearly point measurements, the problem is compounded.

We have considered and experimentally tested four systems for obtaining the wind-weighting function, the relative contribution of the wind as a function of path position. To test the weighting system, we compared our remote optical wind-measurement systems to five Gill anemometers spaced equally along the optical path. A minicomputer performed the calculations on-line.

In the first system, we measured the normalized covariance of each anemometer with the optical wind reading. This system gives a relative weighting and shows the location of maximum and minimum (or even negative) response, but the exact shape of the function is dependent upon the wind variation itself and upon the bandwidth of the fluctuations observed. It is, however, a useful measurement as long as the windspeed and the bandwidth of the measurement are specified.

To remove the bandwidth dependence, one can perform a rudimentary spatial filtering by subtracting the mean of the five anemometer readings from each anemometer. Then one can correlate with the optical signal only the variations in wind at each anemometer location. The measurement for this second system has the disadvantage that the uncorrelated signals give negative results.

A curve-fitting program was used in a third system. The computer was required to find the coefficients for the best fit to the data of an equation of the form $(z(1-z)(C_1+C_2\exp(\frac{-(z-C_3)^2}{2C_4^2}))$.

While the system did work and in principle obtained a weighting function independent of the nature of the wind fluctuations as long as there was enough variation to define the weighting function, there was necessarily some constraint on the allowable form of the weighting function, that is, some preconceived notions of the form of the function were inserted to reduce the amount of computation required.

In the last, and so far most successful system, we evaluated the weighting function along the path directly at the location of each *in situ* measurement. To do this, we give the computer an array of optical and anemometer measurements, requiring it to determine experimentally the weight (factor) by which to multiply each anemometer reading so that

the mean square difference between the sum of these products and the optical reading is a minimum. Thus, this program proceeds directly in a linear fashion to find the weights that we wish to determine with no preconceived notion of the final form.

Using this weighting-factor technique, a second test of the laser-illuminated target system was performed outdoors on a 200-m path as shown in figure 6. Four photodiode receivers were horizontally spaced in the focal plane of the 22-cm diameter receiving objective and were connected as shown. This spatial filter arrangement tended to be most sensitive to

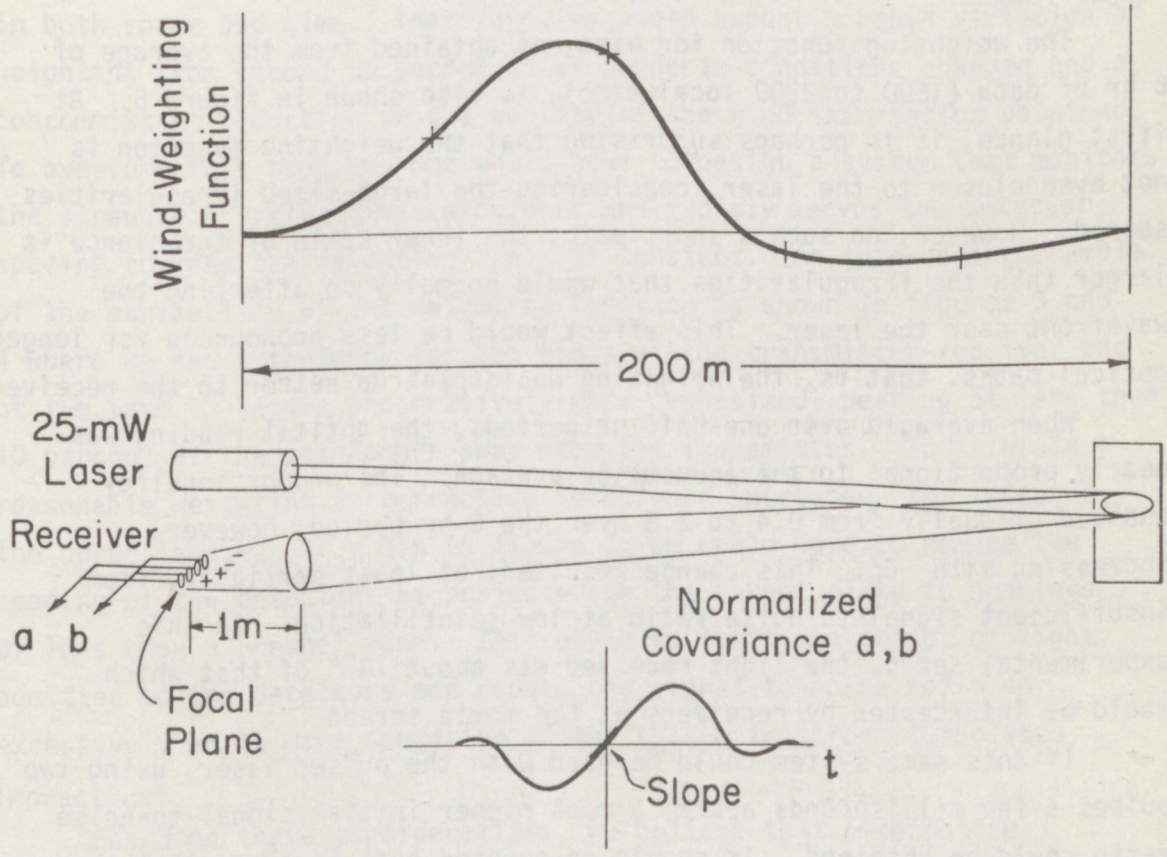

Figure 6. Outdoor test of laser-illuminated target system.

irregularities at the movie screen, approximately 14 cm in diameter, again a larger size than desired but necessary for sufficient signal-to-noise ratio. Anemometers to measure the crosswind component were located at 40-m intervals along the path. The slope of the covariance of the fluctuations of the two filters (which are spaced 90° horizontally for the spatial wavelength sensed) was the optical measurement compared to the anemometers.

The experiment was performed to test the feasibility of the system over a short outdoor path. The spatial size sensed is too large and the pathlength is too short to show the difficulties discussed theoretically. A pulse system of high-peak power would be necessary for experiments at longer ranges.

The weighting function for wind, as obtained from the average of 6 hr of data (1600 to 2200 local time), is also shown in figure 6. At first glance, it is perhaps surprising that the weighting function is not even closer to the laser, considering the large-sized irregularities sensed. However, on such a short path, the inner scale of turbulence is larger than the irregularities that would normally be affecting the wavefront near the laser. This effect would be less pronounced for longer optical paths, that is, the weighting would peak up nearer to the receiver.

When averaged over one-half hr periods, the optical reading was nearly proportional to the anemometer average. The proportionality changed gradually from 0.4 to 2.8 over the 6-hr period, however, increasing with C_N^2. This change resulted, at least partially, from insufficient signal-to-noise ratio at low scintillation. In this experimental setup, the light received was about 10^{-9} of that which would be intercepted by receivers at the movie screen.

If this same system could be used with the pulsed laser, using two pulses a few milliseconds apart, a much higher initial signal-to-noise ratio could be obtained. It should be pointed out, however, that the light requirements for such a system are much higher than those required for a laser-ranging system for several reasons. One reason is that one must look at small details in the laser pattern at the target and cannot

accept the total illumination. Another reason is that one cannot detect just the presence or absence of signal as required for laser ranging, but must also detect small variations of light intensity in the small areas down to a part in 10^{-2} or less at low C_N^2 levels.

5. LIMITATIONS OF THE LASER SYSTEM

From our analysis and experimental work, we find that the single-ended laser-beam crosswind monitor has one serious limitation. Although the weighting function for the wind peaks near the transmitter, a desirable quality when correcting trajectories, the particular weighting function that applies depends strongly on the strength of the temperature turbulence. Atmospheric variables such as this are notoriously nonuniform in both space and time. Therefore, we would expect a rapid variation of weighting from second to second as atmospheric conditions changed and a concommittant reduction in the quality of the wind information obtained. To overcome this problem, one would have to design a system that monitors the strength of refractive turbulence and rapidly servos the detector spacing to keep the weighting function constant. An interesting example of the variability of the weighting function is shown in figures 3 and 4 where we see a tendency for the winds at the transmitter-receiver end of the path to become progressively more emphasized, peaking at less than 10 percent of the pathlength away from the transmitter. To maintain a reasonable weighting as refractive turbulence increased, for instance, the curve labeled $\sigma_\chi^2 = 0.5$ in figure 3, we would have to reduce the spacing of the detectors as projected on the target plane to spacings of less than a Fresnel zone. This would so limit the amount of light admitted to the detectors and reduce the signal-to-noise ratio so excessively as to make operation of the system in strong turbulence impractical.

Based on these considerations, we believe that alternative approaches should be considered. Below, we propose a "passive" system that appears to overcome the specific limitation mentioned above and might provide a simple, practical alternative technique.

6. THEORETICAL ANALYSIS OF THE PASSIVE SYSTEM

The difficulties outlined in the analysis of the active system, that is, a weighting function peaking near the transmitter on all but the shortest ranges, its variability with C_N^2, and the marginal signal-to-noise ratio, are problems arising from the return-path requirement. If the return path itself could be used in a constructive way, then it might not be necessary to observe the effects on the forward path at all or, for that matter, to have a forward path when the ambient illumination is sufficient. We propose to examine one promising technique which will use only the target-to-receiver optical path to determine the transverse winds. In the daytime, this system might well be a passive one, using only the natural illumination of the target.

The way in which such a system might work is similar to the optical measurement of average winds described by Lawrence, Ochs, and Clifford (1972). However, instead of a single-point source of light, there are many sources of light: some with small details, and some large and diffuse. All that should be required of the target is that some detail be present in a size range comparable to a Fresnel zone for the path. (It would not be possible to use the clear blue sky, for example.)

From within this range of spatial sizes of light sources in the target, scintillating light patterns will be drifting across a receiver because of refractive-index irregularities drifting with the wind across the optical path. These patterns are much like those seen in a laser-beam scintillation pattern, except, in this case, there are many patterns superimposed upon one another that are very faint compared to the large amount of nonscintillating background light. Nevertheless, these patterns are detectable, and we expect that a fair degree of control over the wind-weighting function along the path will be realized by spatially filtering the received patterns.

A first step in the mathematical analysis of the passive system is consideration of the wind-weighting function for multiple-point sources. Of course, this step is not an adequate description of the physical problem, but it gives useful insight into the variations of path weighting

that might be expected. A complete analysis, which we will undertake in the next phase of this project, involves the calculation of weighting functions for a source with an arbitrary distribution of spatial Fourier components.

We proceed, following Lee and Harp (1969), and express the total field dE_j, scattered from a differential phase screen at path position s and illuminated by a source at position $(\underset{\sim}{\rho}_j,0)$, in terms of the coordinates in the receiving plane $(\underset{\sim}{\rho},L)$ (see fig. 7)

$$dE_j = 1 - ik\, a_j ds \exp\left[\frac{iK^2 s(L-s)}{2kL}\right] \cos[\underset{\sim}{K}\cdot\underset{\sim}{\rho}(s/L)+\underset{\sim}{K}\cdot\underset{\sim}{\rho}_j(1-s/L)+\underset{\sim}{K}\cdot\underset{\sim}{b}_j] \,. \qquad (13)$$

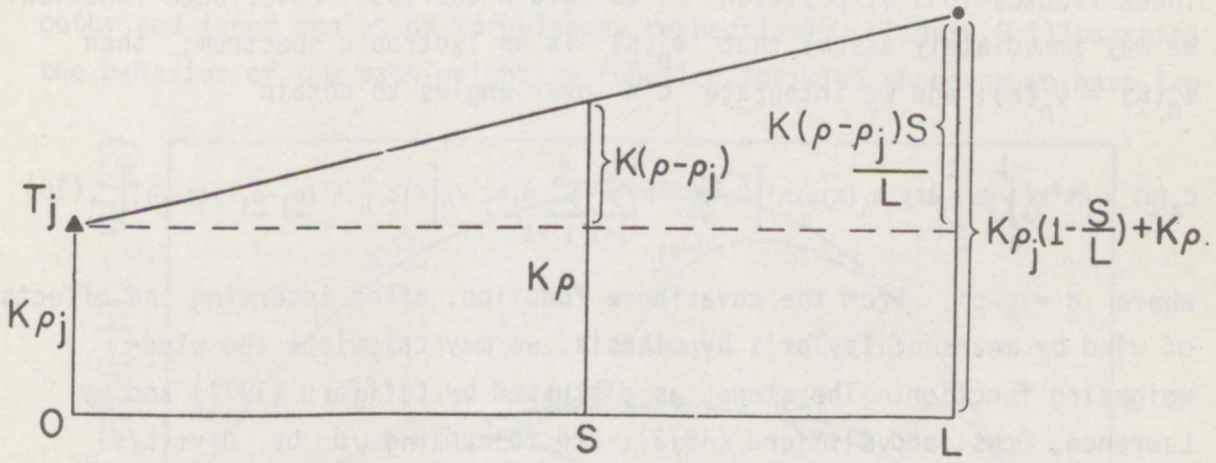

Figure 7. Geometry of the multiple transmitter model.

The quantity a_j is the refractive-index fluctuation of the screen $k=2\pi/\lambda$, where λ is the wavelength of light from the j^{th} source, $\underset{\sim}{K}$ is the two-dimensional spatial frequency of the phase-retarding screen, and $\underset{\sim}{b}_j$ is an arbitrary phase-lag. The effects of scintillation are expressed in the amplitude-perturbation term $dP_j = |dE_j| - 1$. If we retain only terms to the first order, the total amplitude perturbation from N sources dP_a is given by

$$dP_a \simeq \sum_{j=1}^{N} dP_j \quad . \tag{14}$$

Again following Lee and Harp (1969) step by step, we can construct the differential-amplitude covariance function $d\,C_a(\underset{\sim}{\rho},\underset{\sim}{\rho}')$, where

$$dC_a(\underset{\sim}{\rho},\underset{\sim}{\rho}') = 2\pi k^2\, d\underset{\sim}{K}^2 \int_0^L ds\, \Phi_n(\underset{\sim}{K})\, \sin^2\left[\frac{K^2 s(L-s)}{2kL}\right] \sum_{j=1}^{N}\sum_{j'=1}^{N} A_j A_{j'} \cos\left[\underset{\sim}{K}\cdot(\underset{\sim}{\rho}-\underset{\sim}{\rho}')\,\frac{s}{L} + \underset{\sim}{K}\cdot(\underset{\sim}{\rho}_j-\underset{\sim}{\rho}_{j'})\left(1-\frac{s}{L}\right)\right] \quad . \tag{15}$$

In equation (15), $|A_j|^2$ is the intensity of the j^{th} source and $\Phi_n(\underset{\sim}{K})$ is the spectrum of refractive turbulence (Lee and Harp). We now must integrate equation (15) over the entire spectrum of refractive-index fluctuations at position s to obtain the total covariance function. We may immediately assume that $\Phi_n(\underset{\sim}{K})$ is an isotropic spectrum; then $\Phi_n(\underset{\sim}{K}) = \Phi_n(K)$, and we integrate $d^2\underset{\sim}{K}$ over angles to obtain

$$C_a(\underset{\sim}{d}) = 4\pi^2 k^2 \int_0^L ds \int_0^\infty dK K\, \Phi_n(K) \sin^2\left[\frac{K^2 s(L-s)}{2kL}\right] \sum_{j=1}^{N}\sum_{j'=1}^{N} A_j A_{j'} J_o\left[K\left|\underset{\sim}{d}\,\frac{s}{L} + (\underset{\sim}{\rho}_j-\underset{\sim}{\rho}_{j'})\left(1-\frac{s}{L}\right)\right|\right] , \tag{16}$$

where $\underset{\sim}{d} = \underset{\sim}{\rho}-\underset{\sim}{\rho}'$. From the covariance function, after inserting the effects of wind by means of Taylor's hypothesis, we may calculate the wind-weighting function. The steps, as discussed by Clifford (1971) and by Lawrence, Ochs, and Clifford (1972), are to replace $\underset{\sim}{d}$ by $\underset{\sim}{d}+\underset{\sim}{v}\tau(L/s)$ in equation (16), where $\underset{\sim}{v}$ is the wind velocity, to differentiate this expression with respect to time-lag τ, and set $\tau=0$. The resulting expression inside the ds integral will be the wind-weighting function $W(s)$ for the "slope technique" of measuring winds. We perform the above operations after noting that $\partial J_0(x)/\partial x = -J_1(x)$, where J_0 is the zero order and J_1 is the first-order Bessel function of the first kind; then, after dropping the unimportant multiplicative factors, we obtain

$$W(s) = -\sum_{j=1}^{N}\sum_{j'=1}^{N} A_j A_{j'} \frac{\underset{\sim}{m}\cdot[\underset{\sim}{d}(s/L)+(\underset{\sim}{\rho}_j-\underset{\sim}{\rho}_{j'})(1-s/L)]}{|\underset{\sim}{d}(s/L)+(\underset{\sim}{\rho}_j-\underset{\sim}{\rho}_{j'})(1-s/L)|} \int_0^\infty dK K^2 \Phi_n(K) \sin^2\left[\frac{K^2 s(L-s)}{2kL}\right] J_1[K|\underset{\sim}{d}(s/L)+(\underset{\sim}{\rho}_j-\underset{\sim}{\rho}_{j'})(1-s/L)|] , \tag{17}$$

where $\Phi_n^{(1)}(K)$ is defined by $\Phi_n(K) = C_N^2\, \Phi_n^{(1)}(K)$. The quantity $\underset{\sim}{m}$ is a unit vector in the direction of the wind velocity. This general expression can be used for any set of point sources of arbitrary orientation and arbitrary strength. Below we consider certain simple cases.

Equation (17) is, of course, too complex to understand readily. If we now make certain simplifying assumptions such as the detector and transmitter separation are parallel, that is, $\underset{\sim}{d} \| (\underset{\sim}{\rho}_j - \underset{\sim}{\rho}_j')$, limit the number of sources, and insert the usually assumed Kolmogorov spectrum for the turbulent refractivity spectrum (Lawrence, Ochs, and Clifford, 1972), $\Phi_n(K) = 0.033\, C_N^2\, K^{-11/3}$; $L_0^{-1} << K << \ell_0^{-1}$, we obtain the sets of curves shown in figures 8 and 9. The quantities L_0 and ℓ_0 are the outer and inner scales of turbulence, respectively. Figure 8 illustrates the behavior of the path-weighting function for wind whenever we have two

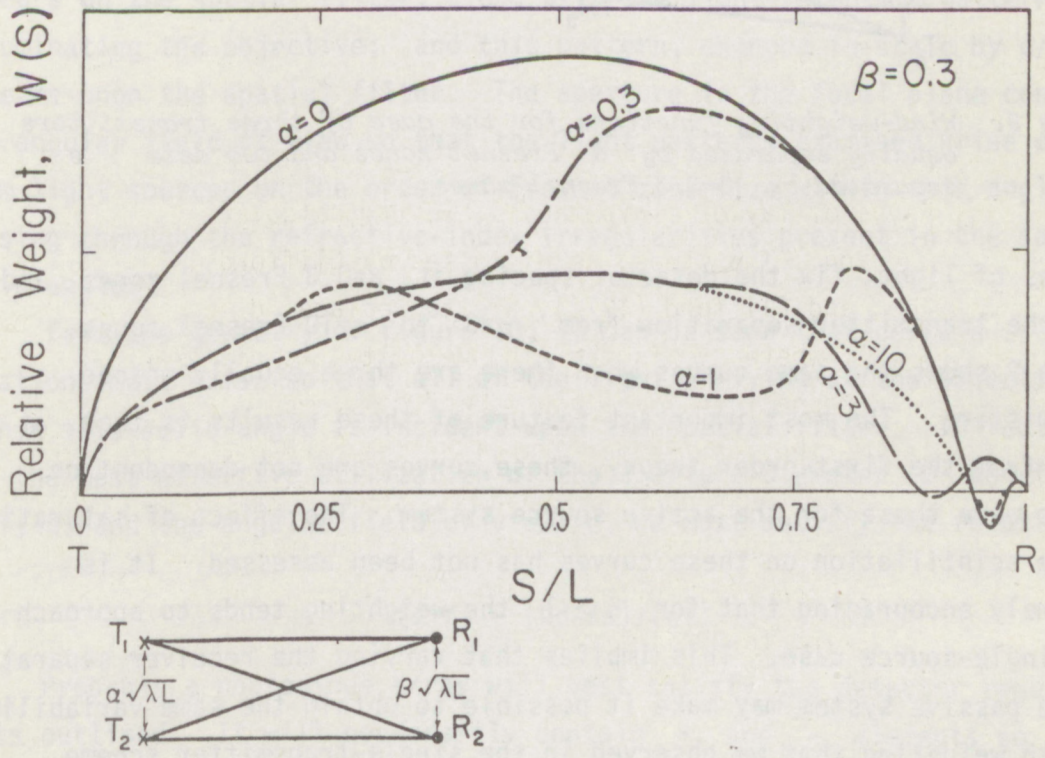

Figure 8. Wind-weighting functions for the case of two transmitters separated by α Fresnel zones and two detectors separated by β=0.3 Fresnel zones.

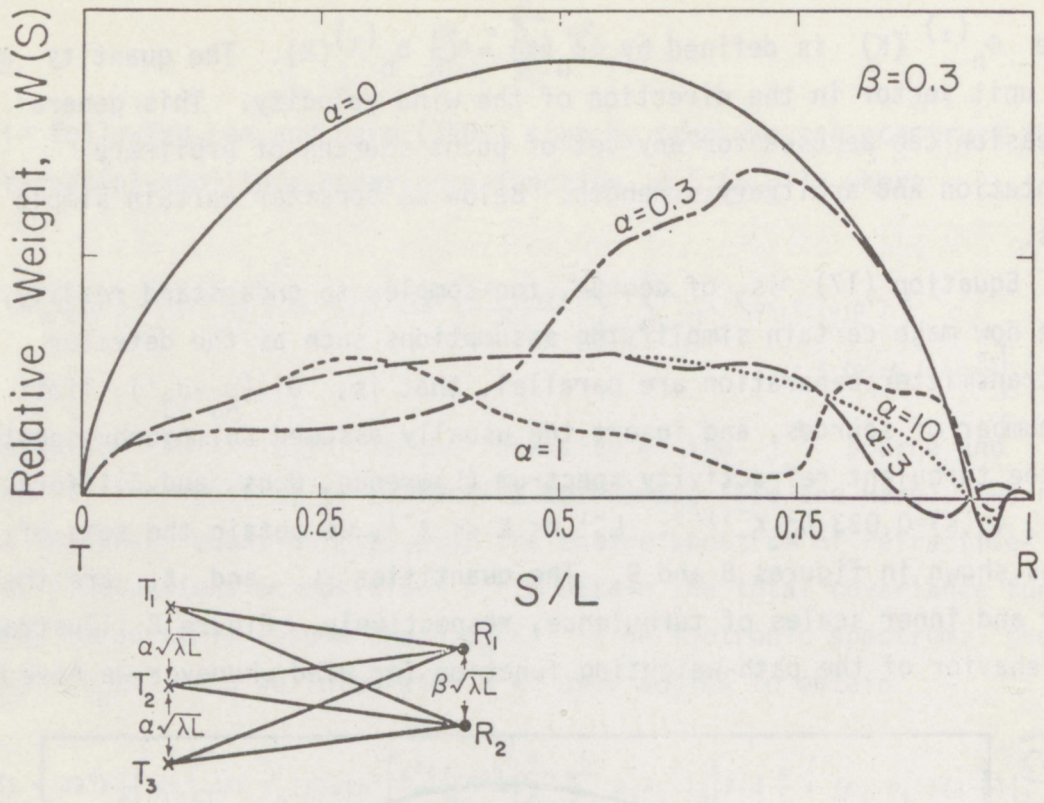

Figure 9. Wind-weighting functions for the case of three transmitters equally separated by α Fresnel zones and two detectors separated by β=0.3 Fresnel zones.

sources of light, fix the detector spacing at $\beta=0.3$ Fresnel zones, and vary the transmitter separation from $\alpha=0$ to $\alpha=10$ Fresnel zones. Figure 9 shows the same curves when there are three equally spaced transmitters. The most important feature of these results is that, at least from the first-order theory, these curves are not dependent on C_N^2 as were those for the active source system. The effect of saturation of the scintillation on these curves has not been assessed. It is extremely encouraging that for $\alpha > 1$ the weighting tends to approach the single-source case. This implies that varying the receiver separation in the passive system may make it possible to obtain the same variability in path weighting that we observed in the single-transmitter scheme (Lawrence, Ochs, and Clifford). These results must be considered tentative at present. We have not fully assessed the validity of our model nor the complications introduced by the saturation effect.

7. RECOMMENDATIONS FOR A PROTOTYPE CROSSWIND MONITOR

It is clear, from the preceding discussions, that a detector, capable of observing accurately very small fluctuations of light in the presence of a high background-light level, would be required. In addition, the detector must be in the form of a spatial filter to observe the proper range of sizes in the pattern so that an appropriate wind-weighting function would be obtained. Another practical requirement is that the field of view must be controlled so that the measured crosswind is over a restricted path. From a signal-to-noise ratio viewpoint, a tradeoff must be made between an acceptable solid-viewing angle Ω and the area A of the receiver because useful light is proportional to $A\Omega$. These requirements suggest the physical arrangement shown in figure 10. We will observe the drifting scintillation pattern over the area of the objective lens. A projection of the objective lens appears on the spatial filter, along with the light-intensity pattern illuminating the objective; and this pattern, changed in scale by d/f, appears upon the spatial filter. The aperture in the focal plane controls the angular field of view so that the light patterns examined arise only from light sources on the order of Fresnel zone size within this angle, passing through the refractive-index irregularities present in the same solid angle.

From the geometry of figure 10, it can be seen that certain relations must exist so that all of the light arriving at the objective within this solid angle is incident upon the spatial filter. In fact, for the most effective utilization of the aperture diameter D and for S, f, d, and the angular field of view ε, we must satisfy the relation

$$(d+f) = (Dd-fs)/(\varepsilon f) \quad .$$

Probably a photodiode array will best satisfy the detector requirements outlined. It will necessarily contain + and - elements so that temporal fluctuations in illumination will be nulled out. However, what will be the exact spatial response of the filter, how it will vary

with range, and whether compensation as a function of C_N^2 or the signal-to-noise ratio will be required must be determined by both theoretical and experimental research.

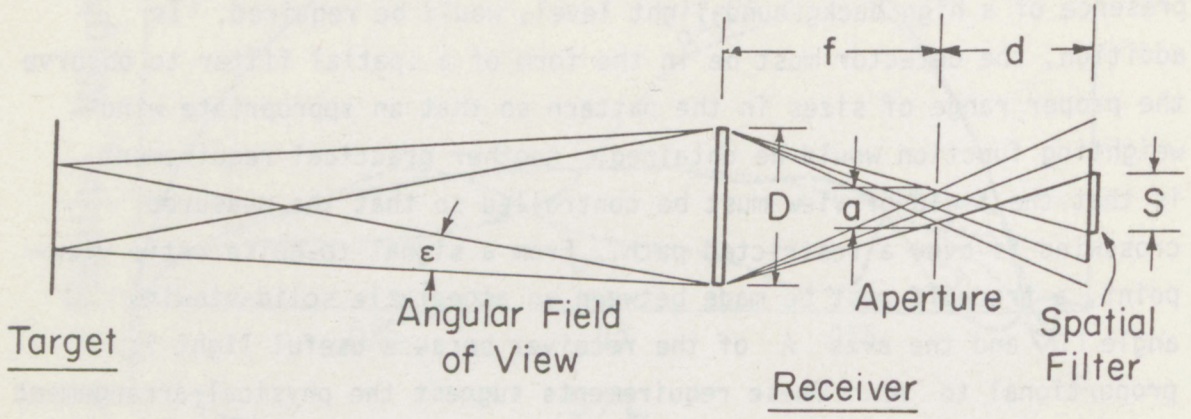

Figure 10. Optical arrangement of passive crosswind monitor.

8. PRELIMINARY EXPERIMENTAL RESULTS

We have made some experimental measurements based upon the passive system. While preliminary, they do show that the general idea is sound. The experiment was conducted along a 500-m path, instrumented with five anemometers spaced equally along the path, and numbered 1 to 5 from the target to the receiver. The target was a large equipment trailer of a dull aluminum color, having little detail on the side except for the outline of several doors. Again, a 22-cm aperture was used. The spatial-filter configuration is illustrated in figure 11. The connections for eight elements are shown; sometimes more elements were used, all connected in the same manner. We measured the slope of the covariance of the fluctuations of a and b and compared this with the readings of the five anemometers. The correlation technique was used to evaluate the relation of this measurement to that of the anemometers. The correlation interval was 20 to 100 sec, and the average of the results of two one-half-hr data runs (1530 to 1630 local time) are shown below.

Spatial wavelength sensed (λ) in cm	No. of filter elements	Correlation with anemometer					Average wind in m/sec	Variance of wind in m/sec	Ratio, optical / anemometer
		1	2	3	4	5			
5.2	16	0.12	0.22	0.46	0.48	0.54	2.1	0.3	1.35
10.4	8	0.26	0.34	0.44	0.32	0.22	2.6	0.2	0.46

The relative ratio of the optical reading to the average-anemometer reading did vary throughout the runs, indicating a more complex dependency than has been assumed in these tests. Note that in the first case, the correlation increases steadily from the target to the receiver, while the correlation peaks at the center of the path in the second case. Thus, it appears that reasonably satisfactory weighting functions can be obtained with some degree of control.

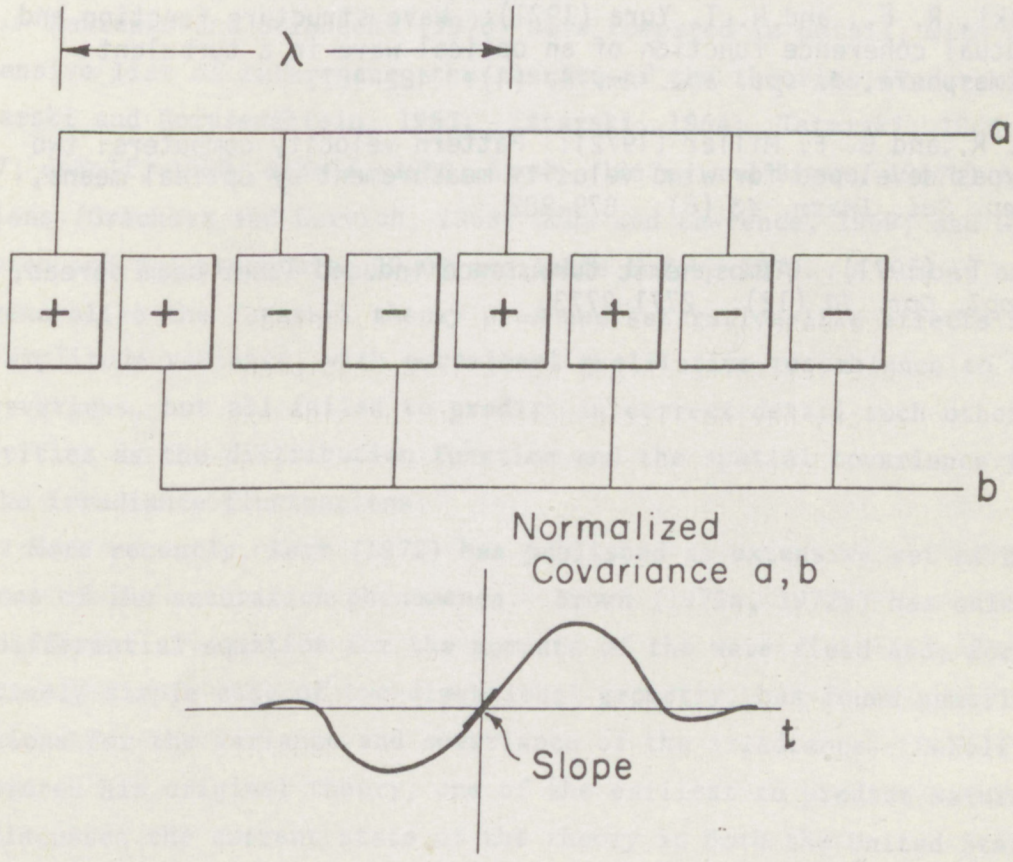

Figure 11. Spatial filter configuration used in the experimental measurement.

9. REFERENCES

Clifford, S. F. (1971): Temporal-frequency spectra for a spherical wave propagating through atmospheric turbulence, *J. Opt. Soc. Am. 61* (10): 1285-1292.

Fried, D. L. (1966): Limiting resolution looking down through the atmosphere, *J. Opt. Soc. Am. 56* (10): 1380-1384.

Fried, D. L. (1967): Aperture averaging of scintillation, *J. Opt. Soc. Am. 57* (2): 169-175.

Lawrence, R. S., G. R. Ochs, and S. F. Clifford (1972): Use of scintillations to measure average wind across a light beam, *Appl. Opt. 11* (2): 239-243.

Lee, R. W., and J. C. Harp (1969): Weak scattering in random media, with applications to remote probing, *Proc. IEEE 57* (4): 375-406.

Lutomirski, R. F., and H. T. Yura (1971): Wave structure function and mutual coherence function of an optical wave in a turbulent atmosphere, *J. Opt. Soc. Am. 61* (4): 482-487.

Ochs, G. R.,and G. F. Miller (1972): Pattern velocity computers: two types developed for wind velocity measurement by optical means, *Rev. Sci. Instr. 43* (6): 879-882.

Yura, H. T. (1971): Atmospheric turbulence induced laser beam spread, *Appl. Opt. 10* (12): 2771-2773.

APPENDIX A.
SATURATION OF OPTICAL SCINTILLATION

A.1 Introduction

The diffraction theory of optical scintillations, suggested by Little (1951) and elaborated by Tatarski (1961, 1971) and Fried (1967), has proven to be remarkably successful in describing the propagation of light through weak and moderate turbulence. However, it has failed to describe the saturation of scintillations that is observed when the integrated amount of turbulence along the path becomes large. It is our purpose in this paper to display some additional observations of the saturation phenomenon and to present a simple, physically base, elaboration of the Tatarski theory that succeeds quantitatively in reproducing the variance and covariance of the observed scintillations.

Lawrence and Strohbehn (1970) have compared in detail, with an extensive list of references, the results of the theories (Tatarski, 1971; Tatarski and Gertsenshtein, 1963; Tatarski, 1964; Tatarski, 1966; deWolf, 1967; deWolf, 1968; deWolf, 1969; Brown, 1967a; and Brown, 1967b) and observations (Gracheva and Gurvich, 1965; Ochs and Lawrence, 1969; and Gracheva, Gurvich, and Kallistratova, 1970) available before 1970. A number of attempts to generalize the Tatarski theory produced saturation-like effects in the log-amplitude variance, with occasional qualitative resemblance to the observations, but all failed to predict in correct detail such other quantities as the distribution function and the spatial covariance function of the irradiance fluctuations.

More recently, Kerr (1972) has published an extensive set of observations of the saturation phenomenon. Brown (1972a, 1972b) has calculated the differential equation for the moments of the wave field and, for the relatively simple case of two-dimensional geometry, has found numerical solutions for the variance and covariance of the irradiance. DeWolf (1973) elaborates his original theory, one of the earliest to predict saturation, and discusses the current state of the theory in both the United States and the Soviet Union. Young (1970) has presented a physically based interpretation of saturation, but his arguments lead to a disappearance

of the fine-scale structure in the scintillation pattern, a conclusion contrary to observations.

The theory that we present in this paper was proposed by Ochs and Clifford (1972) and has been outlined by Clifford (1973). The physical basis for the theory shows why the very smallest scales of irradiance fluctuation persist throughout the saturation region. The equations that result can be solved numerically in the realistic, three-dimensional case and so can be compared in detail with observations. We shall see that the observed variance and covariance are reproduced in detail.

A.2 Experimental Results

We employed a continuous-wave He-Ne laser source with a 3-mW single-mode output at 0.6328 μm. The angular divergence of 2 mrad and the 1-mm transmitter and receiver-aperture size were chosen to approximate a point source for comparison with the spherical-wave scintillation theory (Tatarski, 1961; Fried, 1967; and Livingston, 1972). An earlier paper (Ochs and Lawrence, 1969) describes the characteristics of our optical path and the parameters of the receiver. Supporting measurements of C_T^2 were made in the usual manner (Lawrence, Ochs, and Clifford, 1970), using high-speed platinum resistance thermometers with 10-cm vertical separation. Derivation of C_N^2 from C_T^2 then proceeds from the refractive-index formula.

Figure A1 illustrates the behavior of the log-amplitude standard deviation (square root of the variance), simultaneously observed at 50, 310, 500 and 1000 m, for a 24-hr period. Also shown is the behavior of a point measurement of the refractive-index structure parameter C_N for the same period. All of the curves were smoothed with a 100-sec time constant. The spherical-wave theory (Tatarski, 1961; and Fried, 1967), ignoring the effects of inner scale (Livingston, 1972), predicts a proportionality of the log-amplitude variance, σ_χ^2, to C_N^2 and the path length, L, in the form

$$\sigma_\chi^2 = 0.124\, k^{7/6} L^{11/6} C_N^2 \quad ; \quad L \gg \ell_0^2/\lambda \quad , \tag{A1}$$

where ℓ_0 is the inner scale of turbulence, $k = 2\pi/\lambda$, and λ is the wavelength of the light. Figure A1 clearly shows that on all but the 50-m path,

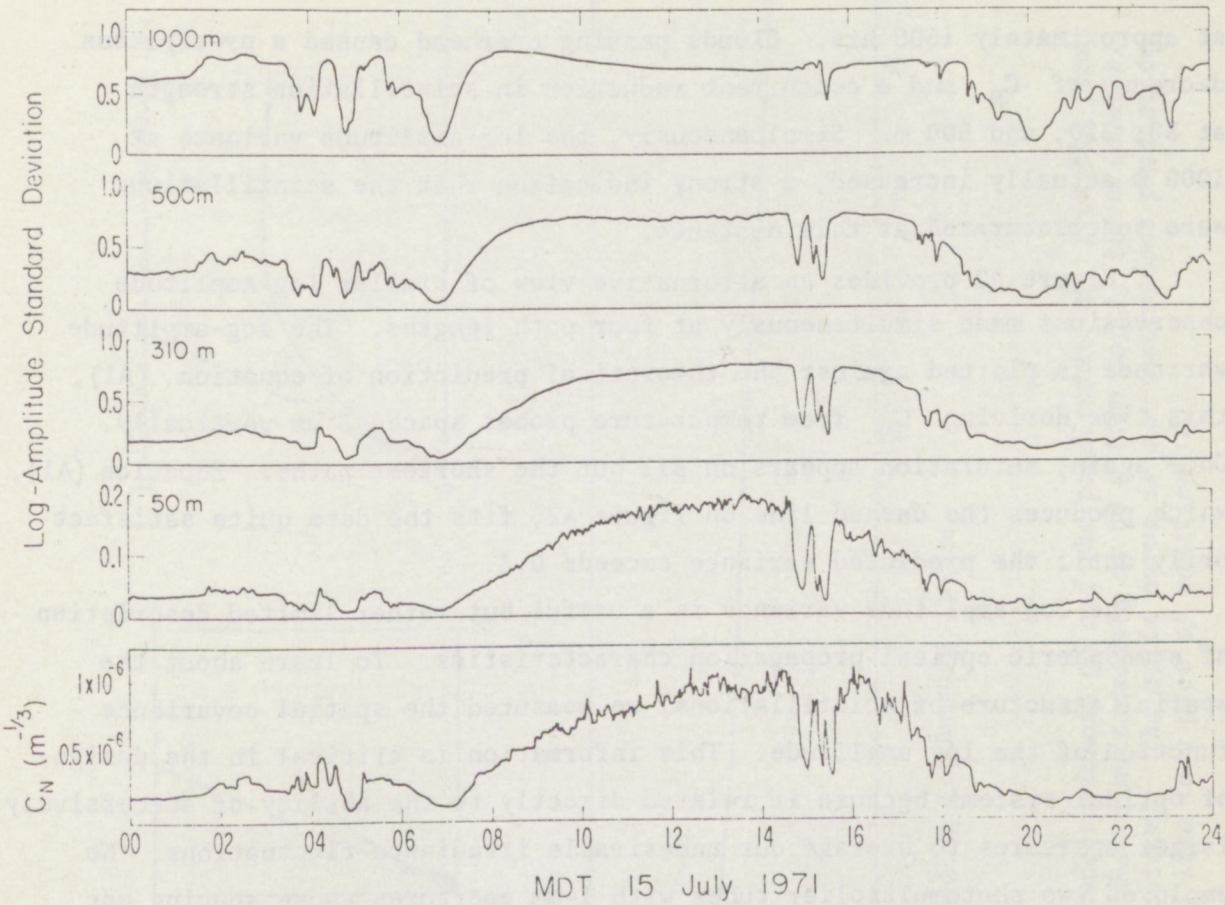

Figure A1. The variation of the square root of the log-amplitude variance at each of four path lengths compared to the refractive-index structure parameter C_N for a 24-hr period. All paths > 50 m show evidence of saturation.

the proportionality breaks down for large values of C_N^2. From our observations, equation (A1) is generally valid as an asymptote for values of σ_χ^2 less than 0.3, though the relation may differ as much as a factor of two over a period of several hours or more. Presumably, different turbulent spectra and nonuniform path distributions of C_N exist for extended periods. When σ_χ^2 exceeds 0.3, the saturation phenomenon occurs and further increases of C_N^2 or of path length fail to produce corresponding increases of σ_χ^2. Continued increases of C_N^2 eventually produce a noticeable decrease of σ_χ^2 (supersaturation) as is shown for the 1000-m path. An interesting consequence of this effect is depicted in figure A1

at approximately 1500 hrs. Clouds passing overhead caused a precipitous decrease of C_N and a concurrent reduction in scintillation strength at 50, 310, and 500 m. Simultaneously, the log-amplitude variance at 1000 m actually increased, a strong indication that the scintillations were supersaturated at this distance.

Figure A2 provides an alternative view of similar log-amplitude observations made simultaneously at four path lengths. The log-amplitude variance is plotted against the theoretical prediction of equation (A1), this time deriving C_N^2 from temperature probes spaced 3 cm vertically. Once again, saturation appears on all but the shortest paths. Equation (A1), which produces the dashed line on figure A2, fits the data quite satisfactorily until the predicted variance exceeds 0.3.

The log-amplitude variance is a useful but rather limited description of atmospheric optical-propagation characteristics. To learn about the spatial structure of scintillations, we measured the spatial covariance function of the log amplitude. This information is critical in the design of optical systems because it related directly to the ability of successively larger apertures to average out undesirable irradiance fluctuations. We employed two photomultiplier tubes with 1-mm apertures whose spacing was varied continuously in a periodic manner. Figure A3 shows a sample of such covariance measurements for a 1-km path during times of weak (bottom) and strong (top) turbulence. The ordinate is the normalized covariance function

$$C_\chi(\underset{\sim}{\rho}) = \frac{1}{2T}\int_{-T}^{T} dt\, \chi(\underset{\sim}{r}+\underset{\sim}{\rho},t)\chi(\underset{\sim}{r},t)/\sigma_\chi^2 \quad , \tag{A2}$$

averaged over an interval $2T = 1$ sec. The abscissa is the detector separation ρ measured in units of a Fresnel zone. Each sweep was made during an interval of approximately 10 min. Sweeps were selected for further analysis on the basis of symmetry; the symmetry indicates the degree of statistical stationarity that prevailed during the measurement.

Figures A4 and A5 summarize such covariance measurements made over 500- and 1000-m propagation paths, respectively. The symbols a through d indicate progressively stronger levels of turbulence as measured by

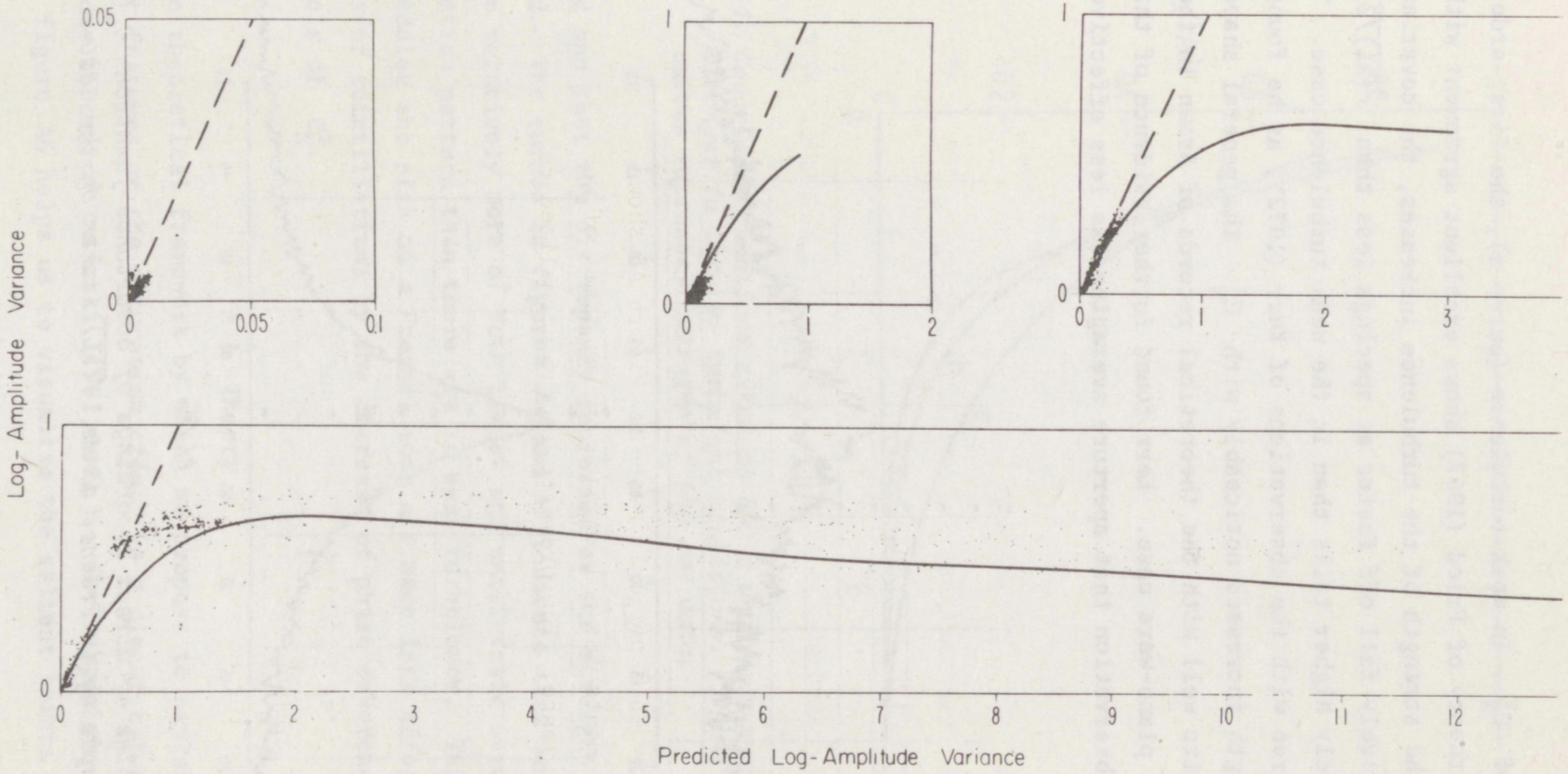

Figure A2. Plots of the observed log-amplitude variance σ_χ^2 and the prediction σ_t^2 from the first order theory. These data were taken simultaneously at 50 m (top left), 250 m (center), 500 m (top right), and 1000 m (bottom). The solid curve is our theoretical prediction from equation (A13). The dashed line is a plot of equation (A1).

higher values of C_N^2. In weak turbulence (curve a), the first-order spherical-wave theory of Fried (1967) shows excellent agreement with the data. As the strength of the turbulence increases, the covariance curves progressively fall off faster at spacings less than $\sqrt{(\lambda L)/2}$ and have progressively higher tails than in the weak turbulence case. The higher tails agree with the observations of Kerr (1972), as he found his correlation length increased noticeably with C_N^2. The general shapes also compare quite well with the theoretical records of Brown in the two-dimensional plane-wave case. Kerr found further evidence of this result in his observation that aperture averaging was less effective than

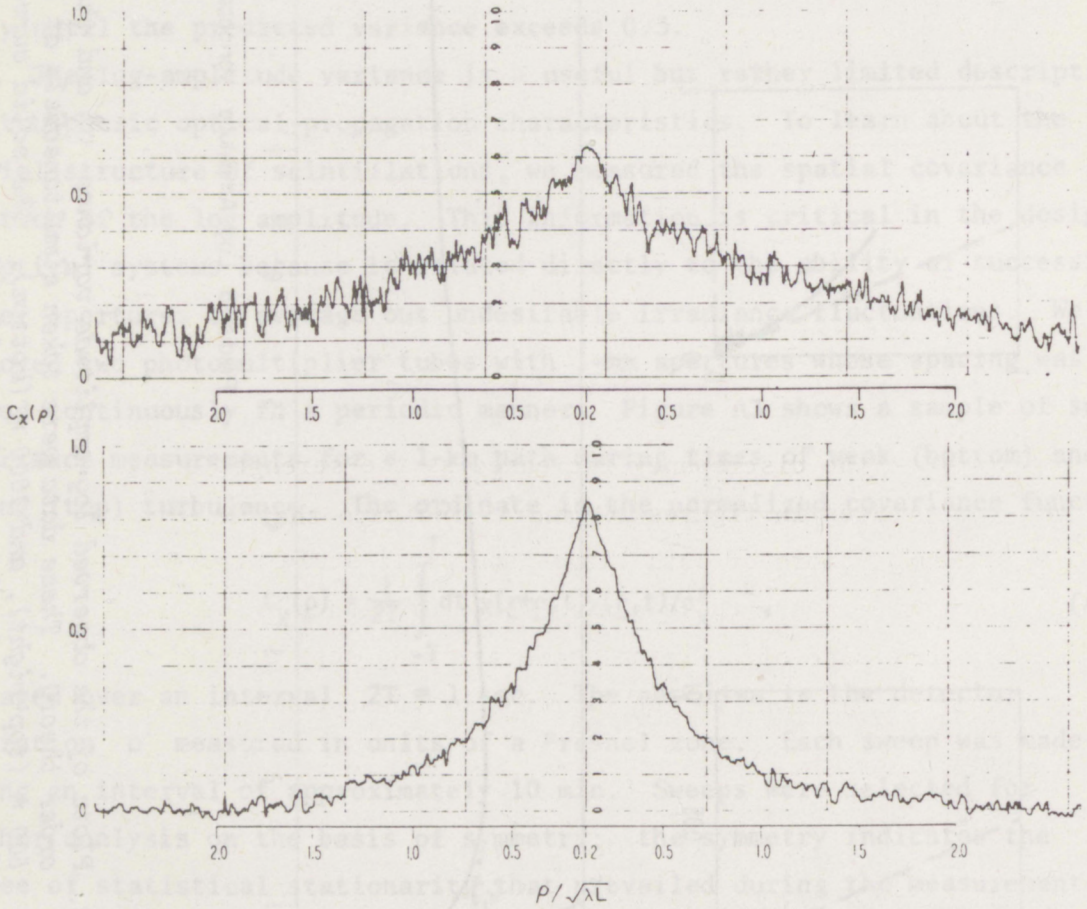

Figure A3. Examples of direct recordings of covariance function $C_\chi(\rho_n)$ and spacing in Fresnel zones $\sqrt{(\lambda L)}$ taken on the 1000-m path.

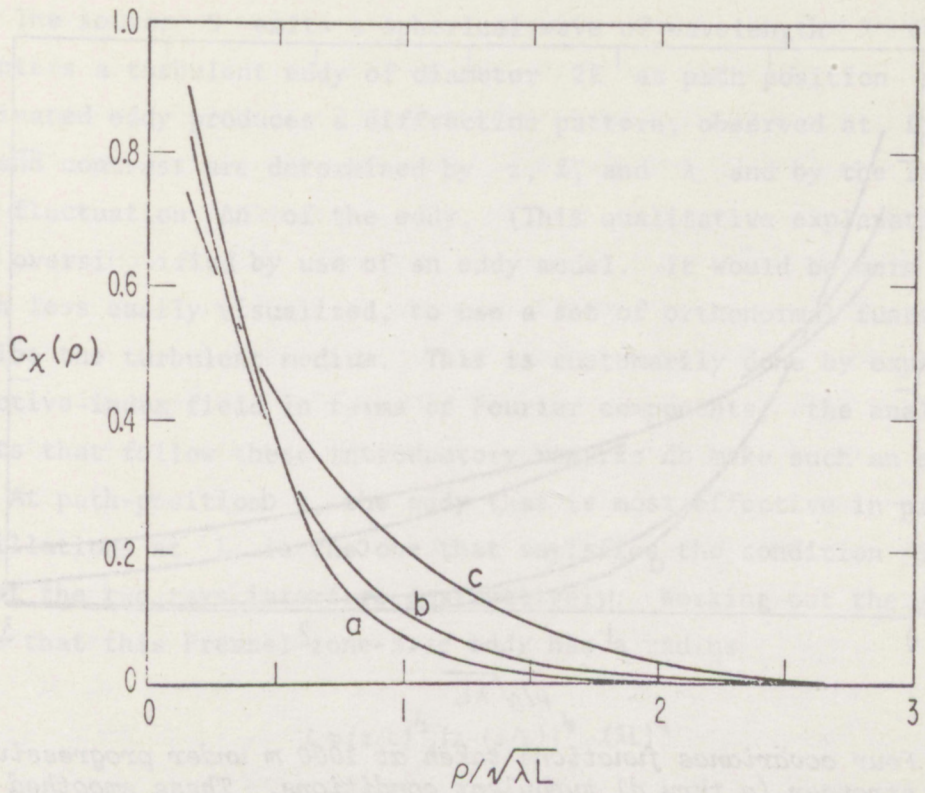

Figure A4. Covariance functions taken at 500 m under progressively stronger (a thru c) turbulent conditions. These smoothed curves represent averages of the raw data.

predicted and that the discrepancy increased as the strength of turbulence increased. The curves in figures A4 and A5 indicate that in strong turbulence there are relatively more of both large- and small-scale structures in the scintillation pattern than there are in weak turbulence. This result occurs because eddies the size of a Fresnel zone are made less effective as producers of scintillations by the decrease of phase coherence induced by high levels of C_N^2.

A.3 Theory

The theoretical framework by which we propose to explain the important features of the saturation effect is a direct extension of the first-order theory of Tatarski (1961, 1971). The simple physical model shown in figure A6 helps us to visualize the salient points of that theory.

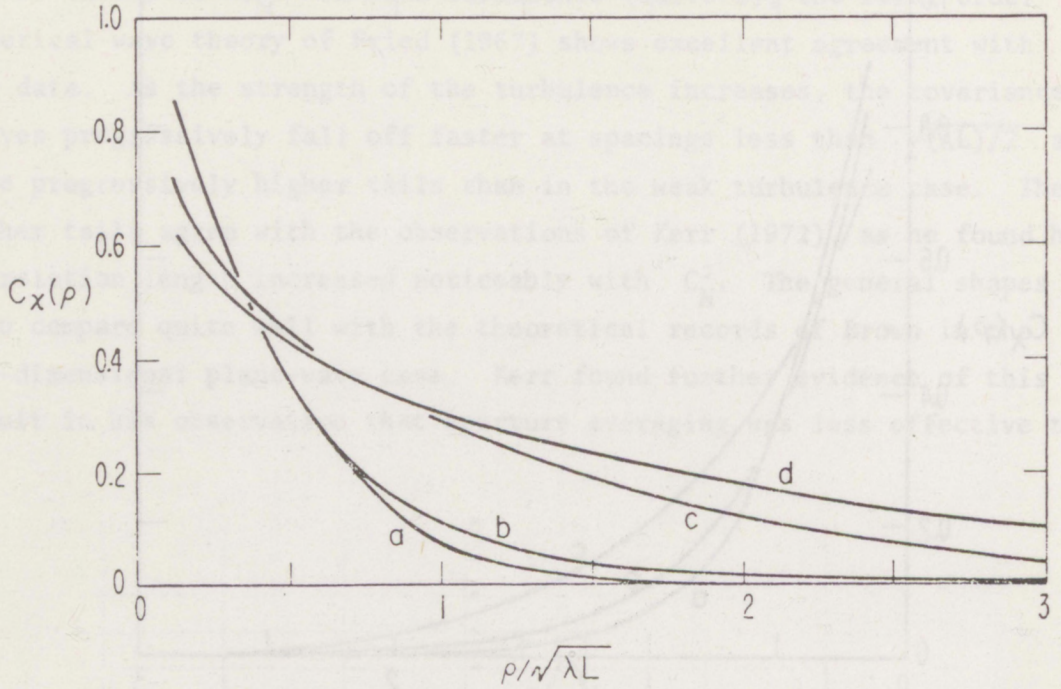

Figure A5. Four covariance functions taken at 1000 m under progressively stronger (a thru d) turbulent conditions. These smoothed curves represent averages of the raw data.

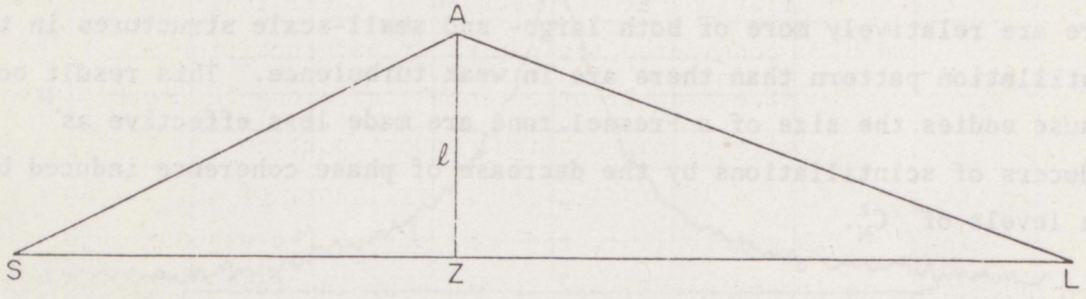

Figure A6. The geometry of the simple eddy model used to explain the salient points of the analysis. The source at S illuminates the eddy of diameter 2ℓ at z and produces scintillations that are observed at position L.

The source S emits a spherical wave of wavelength λ that encounters a turbulent eddy of diameter 2ℓ at path position z. The illuminated eddy produces a diffraction pattern, observed at L, whose size and contrast are determined by z, ℓ, and λ and by the refractive-index fluctuation Δn of the eddy. (This qualitative explanation has been oversimplified by use of an eddy model. It would be more rigorous, though less easily visualized, to use a set of orthonormal functions to describe the turbulent medium. This is customarily done by expanding the refractive-index field in terms of Fourier components; the analytical results that follow these introductory remarks do make such an expansion.)

At path-position z, the eddy that is most effective in producing scintillations at L is the one that satisfies the condition SAL-SL=$\lambda/2$ so that the two rays interfere destructively. Working out the geometry, we see that this Fresnel-zone-size eddy has a radius

$$\ell \approx (z/L)^{1/2}[1-(z/L)]^{1/2} \cdot (\lambda L)^{1/2} \quad . \tag{A3}$$

Smaller eddies at z produce scintillations at path positions $z < L$. Although these scintillations will persist in modified form at L, they contribute less than the others to the variance of irradiance because of the weaker refractivity fluctuation associated in the Kolmogorov spectrum with the smaller eddies. Eddies larger than a Fresnel zone will not produce strong scintillations at L because of their long focal lengths.

So far, we have considered the eddies at path-position z to be acting independently of eddies at other locations along the path. Simple superposition of the effects of such independent portions of the path is, in fact, the basis of the Tatarski first-order theory of scintillation. For sufficiently strong turbulence and long paths, the assumption of independence is no longer useful, as is shown by the failure of the first-order theory to predict saturation. To progress further, we must realize that the eddy at z is illuminated by a wavefront that is no longer spherical but has already been distorted by preceding eddies. In addition, we must realize that succeeding eddies lying between z and L will

affect the wave and will modify the scintillations that might otherwise have been produced as a result of the eddy at z.

Let us first consider how the diffraction pattern of the eddy at z is affected by additional turbulence between the light source and the eddy. To do this, it is convenient to imagine, for the moment, that the eddy is a lens focusing the light on a screen at location L. As the wave passes through the turbulence before reaching the lens, its wavefront is distorted in a random manner. Those distortions having a scale smaller than the lens will cause the resolving power of the lens to diminish and will thus increase the size of the spot observed at L. On the other hand, those distortions larger than the size of the lens will, in effect, be wave tilts and will move the spot on the screen without changing its size. Though it may not be so readily apparent, exactly the same effects will be caused by turbulence lying between the lens and the screen. Thus, it is not important to distinguish between the turbulence on the two sides of the lens, but it is, as we shall see, vitally important to consider separately the effects of the large-scale distortions of the wavefront from the effects of the small-scale distortions.

Returning to the case of the eddy and concentrating particularly upon the Fresnel-zone-size eddies that are the most effective of all the eddies at location z, we must consider the relative lifetimes of the eddies of various sizes. Large eddies persist longer than small eddies, both because of their intrinsic lifetimes and because, for a given cross-wind velocity, they take longer to pass through the line of sight. The small-scale fluctuations in the wavefront, the ones that caused smearing of the focal spot of our lens, change in detail many times during the lifetime of our eddy so they do, in fact, smear the diffraction pattern of our Fresnel-zone-size eddy. On the other hand, the large-scale distortions do not change appreciably during the lifetime of our eddy. Thus, although they may have displaced the diffraction pattern, they can have no effect on the statistics of the scintillations produced by our eddy. Even the smallest details in the scintillation pattern arrive at L unaffected, that is, unsmeared by the large-scale distortions.

To calculate the "smearing" of the details in the scintillation pattern and the concomitant reduction in log-amplitude variance, we use the expression developed by Lutomirski and Yura (1971) for the irradiance profile of an optical beam propagating through turbulence,

$$I(\underset{\sim}{\rho}) = \left[\frac{1+\cos\chi_0}{2\lambda s_0}\right]^2 \int_A \int_A e^{ik(s_1-s_2)+\psi(\underset{\sim}{s}_1)+\psi^*(\underset{\sim}{s}_2)+\psi(\underset{\sim}{r}_1')+\psi^*(\underset{\sim}{r}_2')} u_0(\underset{\sim}{r}_1') u_0^*(\underset{\sim}{r}_2') d^2\underset{\sim}{r}_1' d^2\underset{\sim}{r}_2' . \quad \text{(A4)}$$

Figure A7 shows the definition of each of the geometric quantities. Equation (A4) is the random irradiance profile I that would be observed

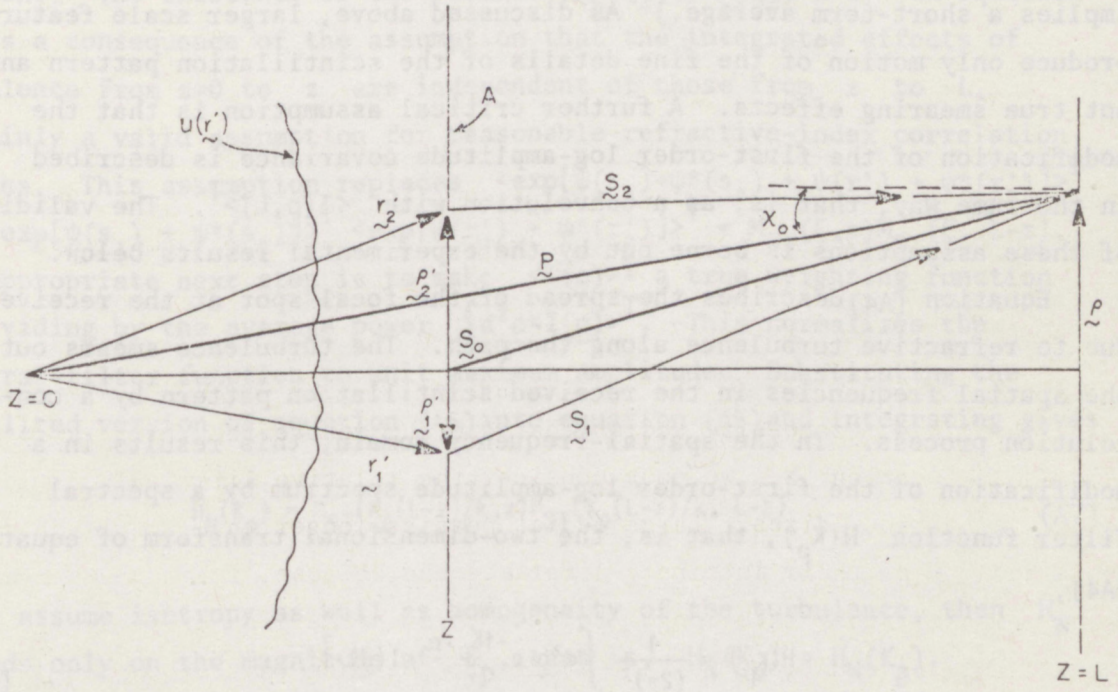

Figure A7. The propagation geometry showing the incident perturbed field $u(\underset{\sim}{r}')$, the scattering at z, and the ultimate field variables at $z=L$.

at location $\underset{\sim}{p} = (\underset{\sim}{\rho}, z)$ from an aperture A illuminated by a random optical field u. The quantity exp (ψ) is the perturbation of the wave field, that is, $u = u_0 \exp(\psi)$, and $k = 2\pi/\lambda$ is the wavenumber of the radiation.

From the model above, we consider each Fourier component of the turbulent temperature field at z as a physical aperture that transmits a turbulence-distorted wave field through the remaining turbulent medium to a receiving plane a distance $(L-z)$ away. A critical assumption, following Young (1970), is that the effects of large integrated turbulence on the statistics of the amplitude fluctuations are adequately taken into account by a convolution of the first-order covariance function with the factor $\langle I(\underset{\sim}{\rho},L)\rangle^T$ or, equivalently, the two-dimensional spectrum of the field parameters should be multiplied by the two-dimensional transform of $\langle I(\underset{\sim}{\rho},L)\rangle^T$. Unlike Young, we believe that the averaging process, described by $\langle\ \rangle^T$, should proceed only over the time and spatial scales relevant to those of the log-amplitude itself. (The superscript T here implies a short-term average.) As discussed above, larger scale features produce only motion of the fine details of the scintillation pattern and not true smearing effects. A further critical assumption is that the modification of the first-order log-amplitude covariance is described in the same way, that is, as a convolution with $\langle I(\underset{\sim}{\rho},L)\rangle^T$. The validity of these assumptions is borne out by the experimental results below.

Equation (A4) describes the spread of the focal spot at the receiver due to refractive turbulence along the path. The turbulence smears out the spatial frequencies in the received scintillation pattern by a convolution process. In the spatial-frequency domain, this results in a modification of the first-order log-amplitude spectrum by a spectral filter function $H(K_p)$, that is, the two-dimensional transform of equation (A4),

$$H(\underset{\sim}{K}_p) = \frac{1}{(2\pi)^2}\int d^2\underset{\sim}{\rho}\, e^{-i\underset{\sim}{K}_p\cdot\underset{\sim}{\rho}}\langle I(\underset{\sim}{\rho})\rangle^T . \qquad \text{(A5)}$$

In equation (A5), K_p is the spatial frequency observed in the receiving plane and $\underset{\sim}{\rho}$ are the coordinates of the observation point in the plane $z=L$. Before performing the operation, we note from figure A7 the relations $\underset{\sim}{s}_1=\underset{\sim}{\rho}-\underset{\sim}{r}_1'$, $\underset{\sim}{s}_2=\underset{\sim}{\rho}-\underset{\sim}{r}_2'$, $s_1^2=(L-z)^2+(\underset{\sim}{\rho}-\underset{\sim}{\rho}_1')^2$, and $s_2^2=(L-z)^2+(\underset{\sim}{\rho}-\underset{\sim}{\rho}_2')^2$, and in equation (A4) make the change of variables $\underset{\sim}{\xi}=\underset{\sim}{\rho}_2'-\underset{\sim}{\rho}_1'$, $2\underset{\sim}{\eta}=\underset{\sim}{\rho}_2'+\underset{\sim}{\rho}_1'$. (These and the following steps are outlined in greater detail by Lutomirski and Yura (1971).) The result of this substitution, the use of the approximation

$s_1 - s_2 \simeq \underset{\sim}{\rho} \cdot (\underset{\sim}{\rho}_2' - \underset{\sim}{\rho}_1')/(L-z) + (\underset{\sim}{\rho}_2'^2 - \underset{\sim}{\rho}_1'^2)/[2(L-z)]$, and the assumption of homogeneous turbulence reduce equation (A4) to the form

$$\langle I(\underset{\sim}{\rho})\rangle^T = \left[\frac{k}{2\pi(L-z)}\right]^2 \int d^2\xi \exp\left\{\frac{ik(\underset{\sim}{\rho}\cdot\underset{\sim}{\xi})}{(L-z)}\right\} M_{ST}(\underset{\sim}{\xi},z) M_{ST}(\underset{\sim}{\xi},L-z) \int d^2\eta \exp\left\{\frac{-ik(\underset{\sim}{\eta}\cdot\underset{\sim}{\xi})}{(L-z)}\right\} u_0^*(\underset{\sim}{\eta}-\underset{\sim}{\xi}/2) u_0(\underset{\sim}{\eta}+\underset{\sim}{\xi}/2). \quad \text{(A6)}$$

The quantity M_{ST} is the appropriate short-term modulation transfer function (MTF) (Fried, 1966). This function is defined (Yura, 1973) by $M_{ST}(\underset{\sim}{r}_1, \underset{\sim}{r}_2) = \langle \exp(\psi(\underset{\sim}{r}_1) + \psi^*(\underset{\sim}{r}_2)\rangle$; for homogeneous turbulence, it depends only on $\underset{\sim}{r}_2 - \underset{\sim}{r}_1$. We consider this function in more detail later. At this point, its only important property is that the function depends on $\underset{\sim}{\xi}$ alone. The existence of the product $M_{ST}(\underset{\sim}{\xi},z) M_{ST}(\underset{\sim}{\xi}, L-z)$ in equation (A6) is a consequence of the assumption that the integrated effects of turbulence from z=0 to z are independent of those from z to L, certainly a valid assumption for reasonable refractive-index correlation lengths. This assumption replaces $\langle \exp[\psi(\underset{\sim}{s}_1) + \psi^*(\underset{\sim}{s}_2) + \psi(\underset{\sim}{r}_1') + \psi^*(\underset{\sim}{r}_2')]\rangle^T$ by $\langle \exp[\psi(\underset{\sim}{s}_1) + \psi^*(\underset{\sim}{s}_2)]\rangle^T \langle \exp[\psi(\underset{\sim}{r}_1') + \psi^*(\underset{\sim}{r}_2')]\rangle^T = M_{ST}(\underset{\sim}{\xi},z) M_{ST}(\underset{\sim}{\xi}, L-z)$. The appropriate next step is to make $\langle I(\underset{\sim}{\rho})\rangle^T$ a true weighting function by dividing by the average power $\int d^2\underset{\sim}{\rho} \langle I(\underset{\sim}{\rho})\rangle^T$. This normalizes the spectral-filter function to unit maximum amplitude. Substituting the normalized version of equation (A6) into equation (A5) and integrating gives

$$H_N(\underset{\sim}{K}_p) = M_{ST}(\underset{\sim}{K}_p(L-z)/k, z) M_{ST}(\underset{\sim}{K}_p(L-z)/k, L-z) \quad . \quad \text{(A7)}$$

If we assume isotropy as well as homogeneity of the turbulence, then H_N depends only on the magnitude of $\underset{\sim}{K}_p$, that is, $H_N(\underset{\sim}{K}_p) = H_N(K_p)$.

Fried (1966) calculated short-term MTF by removing the effects of beam tilt. Tilt can be defined only in terms of the scale size of the aperture upon which the beam impinges. The plane that best fits the two-dimensional phase-fluctuation surface over that aperture then serves as an estimate of tilt and is consequently removed. As discussed previously, this same process can be approximated by high-pass filtering of the spatial-frequency spectrum used to determine MTF so that only scales smaller than the aperture will contribute to the smearing effects described by the short-term MTF. When the aperture is a two-

dimensional spatial frequency (phase screen) and the size of effective aperture is determined by the coherence properties of the incident wave, the separation between large-scale (tilting) and small-scale (smearing) components of the MTF is more difficult to define. During our calculations of the MTF of the wave incident upon the phase-retarding screen, we found that truncating the incident wave's coherence spectrum at spatial frequency proportional to that of the phase screen accomplishes the desired result.

The long-term MTF of a spherical wave propagating through a distance z of homogeneous and isotropic refractive turbulence is given (Lutomirski and Yura, 1971) by

$$M(\rho,z) = \exp\left\{-4\pi^2k^2\int_0^z dz'\int_0^\infty d\kappa'\kappa'\Phi_n(\kappa')\left[1 - J_0\left(\frac{\kappa'\rho z'}{z}\right)\right]\right\}, \qquad \text{(A8)}$$

where Φ_n is the refractive index spectrum and J_0 is the zero-order Bessel function of the first kind. To proceed according to the foregoing argument above, we convert the integral from one over the variable K', the spatial frequencies of the refractive-index spectrum to one over $K_p' = K' z'/z$, that is, an integral over the spatial frequencies in the field of the wavefront variations at a position z produced by eddies at position z'. The variable K_p' represents the spatial wavenumbers in the wavefront distortion that are decreased from those of the refractive-turbulence spectrum by the spherical divergence of the incident wave. Changing variables, we obtain

$$M(\rho,z) = \exp\left\{-4\pi^2k^2\int_0^z dz'(z/z')^2\int_0^\infty dK_p'K_p'\,\Phi_n(K_p'z/z')\left[1-J_0(K_p'\rho)\right]\right\}. \qquad \text{(A9)}$$

To modify equation (A9)to obtain short-term MTF in line with the arguments above, we truncate the integral over wavenumber of the wavefront perturbation below the wavenumber of the refractive index turbulence K and obtain

$$M_{ST}(\rho,z) = \exp\left\{-4\pi^2k^2\int_0^z dz'(z/z')^2\int_{\gamma K}^\infty dK_p'K_p'\,\Phi_n(K_p'z/z')[1-J_0(K_p'\rho)]\right\}. \qquad \text{(A10)}$$

The coefficient in the lower limit is $\gamma=0.35$. This arises because the tilting effects of the irregularities in the incident phase front occur at a spatial frequency somewhat lower than that of the illuminated phase screen. Numerical simulation of a random Kolmogorov phase front impinging on a screen of wavenumber K has indicated that 0.35 K is a reasonable truncation point. A complete and correct theoretical calculation would, of course, produce a smooth high-pass filter in equation (A10).

To complete the analysis, we assume the conventional spectrum for the refractivity fluctuations resulting from Kolmogorov turbulence, that is,

$$\Phi_n(K) = 0.033\, C_N^2\, K^{-11/3},\quad L_0^{-1} << K << \ell_0^{-1} \quad ,$$

and note in the above integral that we may extend the region of integration in equation (A10) to infinity and allow K to vary from zero in the lower limit with negligible error. (The outer scale L_0 may play a significant role here if it is unusually small, i.e., on the order of a few Fresnel zones. Its inclusion in the integral in equation (A10) would result in higher log-amplitude variances as the amount of integrated turbulence increases.) Further, substitution of variables $u=z'/L$ and $\xi=K_p'\rho$ and the performance of the u integration reduces equation (A10) to

$$M_{ST}(\rho,z) = \exp\left\{-0.05\,\pi^2k^2C_N^2z\,\rho^{5/3}\int_{0.35K\rho}^{\infty} d\xi\, \xi^{-8/3}\,[1-J_0(\xi)]\right\} . \qquad \text{(A11)}$$

Returning to equation (A7) and noting the particular form of the z dependence in equation (A11), we see that $M_{ST}(\rho,z)M_{ST}(\rho,L-z)=M_{ST}(\rho,L)$.

We must now write the first-order theory for the log-amplitude covariance function and insert the spectrum modification $M_{ST}(K_p(L-z)/k,L)$. From Lawrence and Strohbehn (1970), the log-amplitude covariance for a spherical wave propagating over a path L through a medium filled with Kolmogorov turbulence is determined by the equation

$$C_\chi(\rho) = 0.132\pi^2k^2L\,C_N^2\int_0^1 du\int_0^\infty dK\, K^{-8/3}J_0(K\rho u)M_{ST}(KLu(1-u)/k,L)\sin^2\left[\frac{K^2u(1-u)L}{2k}\right] . \qquad \text{(A12)}$$

In equation (A12), we have inserted the M_{ST} function and noted that $K_p = Ku$. A change of variables from K to $y = K^2 u(1-u)L/(2k)$ puts this equation in a more suggestive form in terms of the first-order log-amplitude variance, that is, $\sigma_t^2 = 0.124\, K^{7/6} L^{11/6} C_N^2$. With this accomplished, equation (A12) takes the form

$$C_\chi(\rho_n, \sigma_t^2) = 2.95\, \sigma_t^2 \int_0^1 du[u(1-u)]^{5/6} \int_0^\infty dy\, \frac{\sin^2 y}{y^{11/6}} \exp\left\{-\sigma_t^2 [u(1-u)]^{5/6} f(y)\right\} J_0\left[\left(\frac{4\pi y u}{1-u}\right)^{1/2} \rho_n\right] \quad \text{(A13)}$$

where $\rho_n = \rho/\sqrt{(\lambda L)}$ and $f(y)$ is given by

$$f(y) = 7.02\, y^{5/6} \int_{0.7y}^\infty d\xi\, \xi^{-8/3} [1 - J_0(\xi)] \quad . \quad \text{(A14)}$$

Equation (A13) is the equation for the log-amplitude variance and covariance function in the case of strong integrated turbulence $\sigma_t^2 > 0.30$. Asymptotically, it reduces to the first-order result for $\sigma_t^2 \leq 0.30$.

A.4 Comparison with Observations

The results of our theory, equation (A13), produced the saturation curve that is superimposed upon the observed points in figure A2. The relatively low values compared with the experimental points in the linear (unsaturated) region and in the region of high σ_t^2 result from the manner in which we chose to truncate the integral in equation (A10). The scintillation-reducing effects do not occur abruptly as indicated by the form of equation (A10), but more smoothly, so that, for example, Fresnel-zone-size eddies retain some scintillation-producing effect even in strong turbulence. Thus, our abrupt truncation of the integration overstates the effects of strong turbulence on the log-amplitude variance.

A more stringent test of the saturation theory concerns the structure of the scintillation pattern. Figures A3, A4, and A5 show the observed covariance of scintillations; whereas in figure A8, we see a set of theoretical curves that depend on normalized spacing $\rho_n = \rho/\sqrt{(\lambda L)}$ and the first-order log-amplitude variance σ_t^2. Table AI compares the σ_t^2 required for our theory to fit best each of the covariance curves of figures A4 and A5 with the σ_t^2 derived from point temperature measurements. The small rms discrepancies α indicate that observations and theory

agree within the uncertainty of the measurements. Differences between σ_t^2 (temp) and σ_t^2 (theory) arise mostly from the failure of a single-temperature sensor to represent accurately the path-averaged temperature statistics.

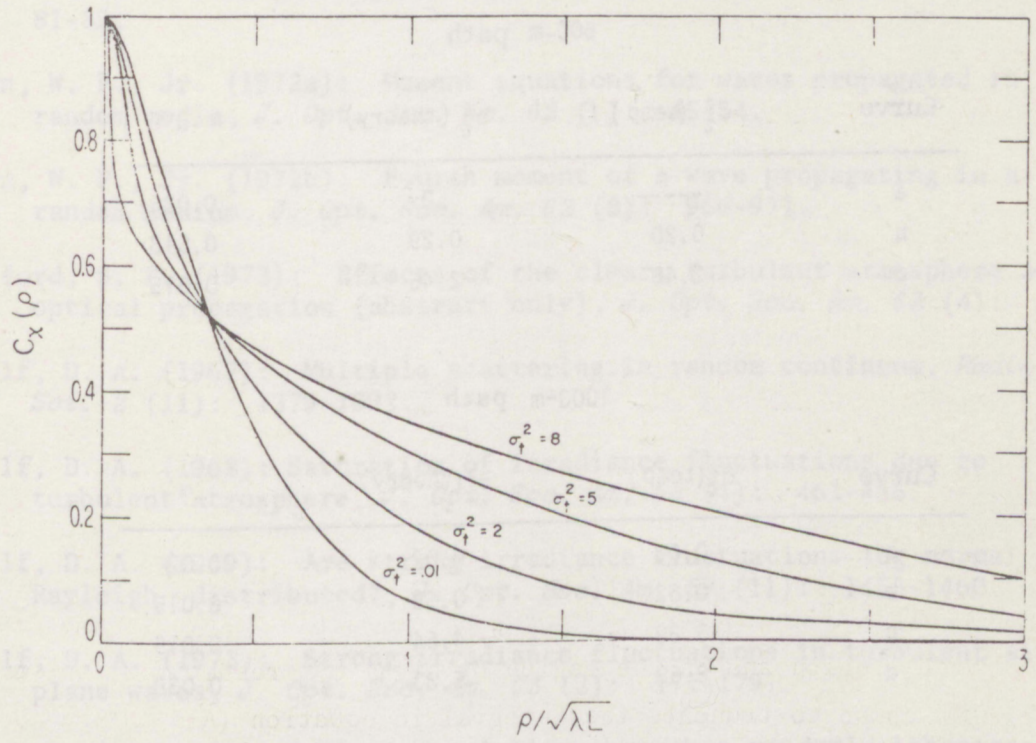

Figure A8. Theoretical covariance curves determined from equation (A13). Each curve results from a different amount of integrated turbulence σ_t^2.

Finally, our model agrees with the observation (Lawrence and Ochs, 1969) that the probability distribution function of irradiance (or amplitude) is log-normal in the saturation region. This statement follows directly from the central-limit theorem because our model of the saturation phenomenon involves only linear filtering (smoothing) of the log amplitude.

In summary, we have proposed a physically based elaboration of the Tatarski theory of propagation through turbulence; numerical results from this model agree with all observed features of the saturation phenomenon.

Table AI.

A comparison of integrated-path refractive turbulence σ_t^2 as determined from temperature measurements and from fitting equation (A13) of our present theory to the observations of figures A4 and A5. Here α is the rms discrepancy in C_χ between the observations and the present theory.

500-m path

Curve	σ_t^2 (temp)	σ_t^2 (theory)	α
a	-----	0	0.026
b	0.20	0.29	0.013
c	2.48	2.46	0.015

1000-m path

Curve	σ_t^2(temp)	σ_t^2(theory)	α
a	0.03	0.02	0.02
b	0.62	0.58	0.015
c	3.89	4.64	0.015
d	8.68	5.83	0.038

A.5 REFERENCES

Brown, W. P., Jr. (1967a): Coherent field in a random medium--effective refractive index, in *Proceedings on the Symposium on Modern Optics*, ed. J. Fox, Polytechnic Press, Brooklyn, N. Y., 717-742.

Brown, W. P., Jr. (1967b): Propagation in random media--cumulative effect of weak inhomogeneities, *IEEE Trans. Ant. Prop. AP-15* (1): 81-89.

Brown, W. P., Jr. (1972a): Moment equations for waves propagated in random media, *J. Opt. Soc. Am. 62* (1): 45-54.

Brown, W. P., Jr. (1972b): Fourth moment of a wave propagating in a random medium, *J. Opt. Soc. Am. 62* (8): 966-971.

Clifford, S. F. (1973): Effects of the clear, turbulent atmosphere on optical propagation (abstract only), *J. Opt. Soc. Am. 63* (4): 471.

deWolf, D. A. (1967): Multiple scattering in random continuum, *Radio Sci. 2* (11): 1379-1392.

deWolf, D. A. (1968): Saturation of irradiance fluctuations due to turbulent atmosphere, *J. Opt. Soc. Am. 58* (4): 461-466.

deWolf, D. A. (1969): Are strong irradiance fluctuations log normal or Rayleigh distributed?, *J. Opt. Soc. Am. 59* (11): 1455-1460.

deWolf, D. A. (1973): Strong irradiance fluctuations in turbulent air: plane waves, *J. Opt. Soc. Am. 63* (2): 171-179.

Fried, D. L. (1966): Optical resolution through a randomly inhomogeneous medium for very long and very short exposures, *J. Opt. Soc. Am. 56* (10): 1372-1379.

Fried, D. L. (1967): Propagation of a spherical wave in a turbulent medium, *J. Opt. Soc. Am. 57* (2): 175-180.

Gracheva, M. E., and A. S. Gurvich (1965): On strong fluctuations of light intensity when propagating in atmospheric layer near the earth, *Izv. Vyssh. Uchebn. Zaved. Radiofiz. 8* (4): 717-724.

Gracheva, M. E., A. S. Gurvich, and M. A. Kallistratova (1970): Measurements of dispersion of 'strong' intensity fluctuations of laser radiation in the atmosphere, *Izv. Vyssh. Uchebn. Zaved. Radiofiz. 13* (1): 56-60.

Kerr, J. R. (1972): Experiments on turbulence characteristics and multi-wavelength scintillation phenomena, *J. Opt. Soc. Am. 62* (9): 1040-1049.

Lawrence, R. S., and J. W. Strohbehn (1970): A survey of clear-air propagation effects relevant to optical communications, *Proc. IEEE 58* (10): 1523-1545.

Lawrence, R. S., G. R. Ochs, and S. F. Clifford (1970): Measurements of atmospheric turbulence relevant to optical propagation, *J. Opt. Soc. Am. 60* (6): 826-830.

Little, C. G. (1951): A diffraction theory of the scintillation of stars on optical and radio wavelengths, *Monthly Notices Roy. Astron. Soc. 111* (3): 289-302.

Livingston, P. M. (1972): Proposed method of inner scale measurement in a turbulent atmosphere, *Appl. Opt. 11* (3): 684-687.

Lutomirski, R. F., and H. T. Yura (1971a): Propagation of a finite optical beam in an inhomogeneous medium, *Appl. Opt. 10* (7): 1652-1658.

Lutomirski, R. F., and H. T. Yura (1971b): Wave structure function and mutual coherence function of an optical wave in a turbulent atmosphere, *J. Opt. Soc. Am. 61* (4): 482-487.

Ochs, G. R., and R. S. Lawrence (1969): Saturation of laser-beam scintillation under conditions of strong atmospheric turbulence, *J. Opt. Soc. Am. 59* (2): 226-227.

Ochs, G. R., and S. F. Clifford (1972): Saturation of optical-amplitude scintillation at 0.6328-μm wavelength (abstract only), *J. Opt. Soc. Am. 62* (5): 728-729.

Tatarski, V. I. (1961): *Wave Propagation in a Turbulent Medium*, translated by R. S. Silverman, McGraw-Hill Book Co., Inc., New York, N.Y. 285 pp.

Tatarski, V. I., and M. E. Gertsenshtein (1963): Propagation of waves in a medium with strong fluctuation of the refractive index, *Sov. Phys.-JETP* (English transl.) *17* (2): 458-463.

Tatarski, V. I. (1964): Propagation of electromagnetic waves in a medium with strong dielectric-constant fluctuations, *Sov. Phys.-JETP* (English transl.) *19* (4): 946-953.

Tatarski, V. I. (1966): On strong fluctuations of light wave parameters in a turbulent medium, *Sov. Phys.-JETP* (English transl.) *22* (5): 1083-1088.

Tatarski, V. I. (1971): *The Effects of the Turbulent Atmosphere on Wave Propagation*, (translated from the Russian by the Israel Program for Scientific Translations; originally published in 1967), U.S. Dept. of Commerce, Nat. Tech. Info. Ser., Springfield, Va. 472 pp.

Young, A. T. (1970): Saturation of scintillation, *J. Opt. Soc. Am. 60* (11): 1495-1500.

Yura, H. T. (1973): Short-term average optical-beam spread in a turbulent medium, *J. Opt. Soc. Am. 63* (5): 567-572.